J. Am. Chem. Soc. **1991**, *113*, 4173–4184 4173

Assessment of the "T_1 Criterion" for Distinguishing between Classical and Nonclassical Transition-Metal Hydrides: Hydride Relaxation Rates in Tris(triarylphosphine)osmium Tetrahydrides and Related Polyhydrides

Peter J. Desrosiers,[1a,b] Lisheng Cai,[1a] Zerong Lin,[1a] Rosalie Richards,[1a,b] and Jack Halpern*,[1a]

Contribution from the Departments of Chemistry, The University of Chicago, Chicago, Illinois 60637, and The University of the Virgin Islands, Charlotte-Amalie, St. Thomas, U.S. Virgin Islands 00802. *Received September 4, 1990*

Abstract: $[OsH_4(PTol_3)_3]$ (1, Tol = *p*-tolyl) and a series of related isotopomers $[OsH_xD_{4-x}\{P(Tol\text{-}o\text{-}d_2)_3\}_3]$ (x = 1, 2, 3, and 4) were prepared and hydride spin–lattice relaxation times, T_1, determined as a function of temperature for each one. From these measurements the contributions to the relaxation rates of the hydride ligands from the other hydrides and from the ortho protons of the triarylphosphine ligands were determined to be 62% and 33%, respectively. Taking account of these, as well as of the contributions from the phosphorus nuclei (2%) and osmium nucleus (<0.5%), the calculated relaxation rate, 4.17 s^{-1} (T_1(min) = 238 ms at 500 MHz) agrees to within 3% with the measured one, 4.29 s^{-1}. Similar calculations were performed on 33 other "classical" hydrides for which the relaxation rates at 500 MHz ranged from 1.67 to 9.09 s^{-1} (T_1(min) at 500 MHz from 670 to 110 ms). For the majority of these, the calculated and observed relaxation rates agree to within 10%, with contributions from dipole–dipole interactions with nuclei other than metal-coordinated protons accounting for more than 60% of the observed relaxation rates. Such contributions, typically, have been neglected in previous interpretations of T_1(min). For "nonclassical" hydrides, i.e. those containing η^2-H_2 ligands, agreement between observed and calculated relaxation rates was less satisfactory. Even in such cases dipole–dipole interactions with nuclei other than metal-coordinated protons account for up to 25% of the observed relaxation rates emphasizing that, in general, such interactions cannot be ignored. There is an overlap between the range of T_1(min) values found for classical and nonclassical polyhydrides. For several polyhydrides of undetermined structure, such as $[OsH_5(PTol_3)_3]^+$, $[RuH_4(PCy_3)_3]$, and $[RuH_6(PCy_3)_2]$ (including some that had previously been assigned nonclassical structures on the basis of the "T_1 criterion"), T_1(min) is shown to be consistent with both classical and nonclassical structures.

Introduction

Although it has been suggested that many transition-metal polyhydride complexes have "nonclassical" structures, i.e., contain η^2-H_2 ligands, only in a few cases have such structures been unequivocally demonstrated, sometimes by NMR but most convincingly by X-ray crystallography or neutron diffraction.[2] More commonly, fluxional behavior, often down to the lowest attainable temperatures, precludes an unambiguous structural assignment based on NMR and it is necessary to resort, instead, to "indirect" evidence. One approach that has been proposed,[3a] and extensively applied, to discriminate between "classical" and "nonclassical" (i.e. η^2-H_2 containing) structures in such cases is based on measurement of the spin–lattice relaxation time, T_1, of the hydride ligands.[2-7]

The basis for this approach, as originally formulated, is the assumption that relaxation of the NMR signals of the coordinated protons is due entirely to dipole–dipole interactions with the other coordinated protons (hydrides)[8a] and that the short H–H separation of η^2-H_2 ligands will give rise to distinctively short T_1 relaxation times which, in turn, may be used to identify such ligands. In this paper we examine the validity and limitations of this criterion.

In this connection we note that other recent studies[3d,6a] also call into question the validity of the original version of the proposed application of this "T_1 criterion" and that several of the molecules originally "identified" as having nonclassical structures according to this criterion, for example, $[ReH_5(PMePh_2)_3]$[6c] and $[ReH_7(dppe)]$,[3a,8b] subsequently have been demonstrated to be classical polyhydrides.[9]

As originally proposed,[3a] the "T_1 criterion" for distinguishing between "classical" and "nonclassical" hydrides was based on the distinction of whether T_1(min) (i.e., the minimum value of T_1 when the temperature is varied) was shorter than 80 ms (nonclassical) or greater than 150 ms (classical) at 250 MHz. (T_1(min) is proportional to the magnetic field strength, so that these values correspond to 160 and 300 ms at 500 MHz, etc.) Recent studies have revealed several examples of polyhydrides that apparently violate this criterion as originally formulated, e.g., $[ReH_7(dppe)]$ (T_1(min) = 67 ms at 250 MHz) was originally "identified" as nonclassical on the basis of its T_1(min) value[3a] but subsequently has been shown by neutron diffraction to have a classical structure.[9] This has raised questions about the validity of the T_1 criterion and led to recognition that, at the very least, the limit

---

(1) (a) The University of Chicago. (b) The University of the Virgin Islands.

(2) For example: (a) Kubas, G. J.; Ryan, R. R.; Swanson, B. I.; Vergamini, P. J.; Wasserman, H. J. *J. Am. Chem. Soc.* **1984**, *106*, 451–452. (b) Morris, R. H.; Sawyer, J. F.; Shiralian, M.; Zubkowski, J. D. *J. Am. Chem. Soc.* **1985**, *107*, 5581–5582. (c) Ricci, J. S.; Koetzle, T. F.; Bautista, M. T.; Hofstede, T. M.; Morris, R. H.; Sawyer, J. F. *J. Am. Chem. Soc.* **1989**, *111*, 8823–8827. (d) Van Der Sluys, L. S.; Eckert, J.; Eisenstein, O.; Hall, J. H.; Huffman, J. C.; Jackson, S. A.; Koetzle, T. F.; Kubas, G. J.; Vergamini, P. J.; Caulton, K. G. *J. Am. Chem. Soc.* **1990**, *112*, 4831–4841. (e) Cotton, F. A.; Luck, R. L. *J. Chem. Soc., Chem. Commun.* **1988**, 1277–1278.

(3) (a) Hamilton, D. G.; Crabtree, R. H. *J. Am. Chem. Soc.* **1988**, *110*, 4126–4133 and references therein. (b) Luo, X.-L.; Crabtree, R. H. *J. Am. Chem. Soc.* **1990**, *112*, 4813–4821. (c) Crabtree, R. H. *Acc. Chem. Res.* **1990**, *23*, 95–101. (d) Luo, X.-L.; Crabtree, R. H. *Inorg. Chem.* **1989**, *28*, 3775–3777.

(4) (a) Arliguie, T.; Chandret, B.; Morris, R. H.; Sella, A. *Inorg. Chem.* **1988**, *27*, 598–599. (b) Bautista, M. T.; Earl, K. A.; Maltby, P. A.; Morris, R. H.; Schweitzer, C. T.; Sella, A. *J. Am. Chem. Soc.* **1988**, *110*, 7031–7036.

(5) Kubas, G. J. *Acc. Chem. Res.* **1988**, *21*, 120–128.

(6) (a) Cotton, F. A.; Luck, R. L. *J. Am. Chem. Soc.* **1989**, *111*, 5757–5761. (b) Cotton, F. A.; Luck, R. L. *Inorg. Chem.* **1989**, *28*, 2181–2186. (c) Cotton, F. A.; Luck, R. L. *Inorg. Chem.* **1989**, *28*, 6–8. (d) Cotton, F. A.; Luck, R. L.; Root, D. R.; Walton, R. A. *Inorg. Chem.* **1990**, *29*, 43–47.

(7) (a) Chinn, M. S.; Heinekey, M. *J. Am. Chem. Soc.* **1987**, *109*, 5865–5867. (b) Kim, Y.; Deng, H.; Meek, D. W.; Wojcicki, A. *J. Am. Chem. Soc.* **1990**, *112*, 2798–2800. (c) Collman, J. P.; Wagenenknecht, P. S.; Hembre, R. T.; Lewis, N. S. *J. Am. Chem. Soc.* **1990**, *112*, 1294–1295. (d) Amendola, P.; Antoniutti, S.; Albertin, G.; Bordignon, E. *Inorg. Chem.* **1990**, *29*, 318–324.

(8) (a) The term "hydride" is used to designate protons coordinated to the metal irrespective of the nature of the bonding (i.e., terminal or η^2-H_2). (b) dppe = 1,2-bis(diphenylphosphino)ethane; OEP = octaethylporphyrin; depe = 1,2-bis(diethylphosphino)ethane; tetraphos = $PPh_2(CH_2CH_2PPh)_2CH_2CH_2PPh_2$; Cyttp = $PhP(CH_2CH_2CH_2PCy_2)_2$.

(9) (a) For the neutron structure of $[ReH_5(PMePh_2)_3]$ see: Emge, T. J.; Koetzle, T. F.; Bruno, J. W.; Caulton, K. G. *Inorg. Chem.* **1984**, *23*, 4012–4017. (b) For the neutron structure of $[ReH_7(dppe)]$ see: Howard, J. A. K.; Mason, S. A.; Johnson, O.; Diamond, I. C.; Crennel, S.; Keller, P. A.; Spencer, J. L. *J. Chem. Soc., Chem. Commun.* **1988**, 1502–1503.

0002-7863/91/1513-4173$02.50/0

of T_1(min) values that must be considered as compatible with "classical" structures is much lower than originally proposed. However, a satisfactory quantitative assessment of the validity and limitations of the T_1 method still is lacking and, in this paper, we attempt to provide such an assessment, notably by examining the factors that contribute to metal-coordinated proton relaxation in $[OsH_4(PTol_3)_3]$ (Tol = *p*-tolyl) and related polyhydrides.

For T_1 measurements to be used in the way that they have been, to conclude that a polyhydride has a "nonclassical" structure, *two* conditions must be satisfied, namely (1) only dipole–dipole interactions may contribute to relaxation, and (2) the T_1(min) values *must be inconsistent with classical structures.* If dipole–dipole interactions with protons other than those directly coordinated to the metal, or with other nuclei, contribute to relaxation, these contributions also must be considered.

Theory of Dipole–Dipole Relaxation

For a proton, the relaxation rate due to homonuclear dipole–dipole interactions, R_{HH} (the reciprocal of the spin–lattice relaxation time, T_1, when ^1H–^1H dipole–dipole interaction is the only mechanism of relaxation), is given by eq 1, where γ_H is the

$$R_{HH} = \frac{3\gamma_H{}^4\hbar^2}{10r^6}\left\{\frac{\tau_c}{1 + \tau_c{}^2\omega^2} + \frac{4\tau_c}{1 + 4\tau_c{}^2\omega^2}\right\} \qquad (1)$$

gyromagnetic ratio of the proton, ω is the Larmor frequency, r is the internuclear distance (Å) separating the dipoles, and τ_c is the rotational correlation time, which is related to the rate of tumbling in solution and hence decreases with increasing temperature.[10] When $\omega^2\tau_c{}^2 \ll 1$ (the fast motion regime) the term in brackets reduces to $5\tau_c$. In this limit R_{HH} is proportional to τ_c and independent of magnetic field strength. When $\omega^2\tau_c{}^2 \gg 1$ (the slow motion regime), the term in brackets reduces to $2/\omega^2\tau_c$ and R is inversely dependent on both τ_c and ω^2. Thus, with increasing temperature, T_1 (i.e., $1/R_{HH}$) decreases, passes through a minimum, and then increases.

The minimum value of T_1 (T_1(min)) is proportional to the magnetic field strength with the minimum occurring at higher temperature with increasing field strength. This can be most readily seen by differentiating eq 1 with respect to τ_c (eq 2) and setting the derivative $\partial R_{HH}/\partial\tau_c$ equal to zero to yield a polynomial of $\omega\tau_c$ (eq 3). Solving for $\omega\tau_c$ gives $\omega\tau_c = 0.6158$. Since ω is

$$\frac{\partial R_{HH}}{\partial\tau_c} = \frac{3\gamma_H{}^4\hbar^2}{10r^6}\left\{\frac{1 - \tau_c{}^2\omega^2}{(1 + \tau_c{}^2\omega^2)^2} + \frac{4(1 - 4\tau_c{}^2\omega^2)}{(1 + 4\tau_c{}^2\omega^2)^2}\right\} \qquad (2)$$

$$32\omega^6\tau_c{}^6 + 20\omega^4\tau_c{}^4 + \omega^2\tau_c{}^2 - 5 = 0 \qquad (3)$$

proportional to the magnetic field strength, τ_c(min) (the value of τ_c at which $\partial R_{HH}/\partial\tau_c = 0$) is inversely proportional to the magnetic field strength. Qualitatively, the temperature at which T_1 is a minimum increases with magnetic field strength because the rate of tumbling needed to match the Larmor frequency is greater. Since the denominators in the bracketed term of eq 1 contain only constants and multiples of $(\omega\tau_c)^2$ and are therefore independent of magnetic field strength when T_1 is a minimum, the relaxation rate is a linear function of τ_c(min), and T_1(min) is a linear function of magnetic field strength.

The Larmor frequency of a proton in a magnetic field of 11.7 T (unless otherwise stated all relaxation rates and values of T_1(min) reported in this paper are those in a field of 11.7 T, the magnetic field of a 500-MHz spectrometer) is 3.142×10^9 s^{-1}, leading to a value of τ_c of 1.960×10^{-10} s at T_1(min). Substituting this value of τ_c(min) into eq 1 and evaluating the constants yields eq 4, relating the relaxation rate (s^{-1}) at 500 MHz and the internuclear distance in Å (throughout this paper relaxation rates, $R = [T_1(\text{min})]^{-1}$, are used in preference to T_1(min) because they are additive). Similar expressions for the relaxation rate due to heteroatom–proton interactions were obtained with eq 5, where γ_X is the gyromagnetic ratio of the heteronucleus,[11] ω_+ and ω_- are defined as $\omega_H + \omega_X$ and $\omega_H - \omega_X$ respectively, and S is the nuclear spin of X. Substituting τ_c(min) for τ_c into eq 5[12] and evaluating the constants leads to a series of equations of the general form of eq 6. Table I lists the values of γ_X and K_X for the heteroatom nuclei used in this study.

$$R_{HH} = 77.51\ \text{Å}^6\ \text{s}^{-1}/r^6 \qquad (4)$$

Table I. Gyromagnetic Ratios (γ) and K_X (=R_{HX} at 500 MHz × r^6, Eq 6) for Various Nuclei

nucleus	abundance, %	γ, G^{-1} s^{-1}	K_X, (Å^6 s^{-1})
^1H	99.985	2.675×10^4	77.51
^2H	0.015	4.107×10^3	4.875
^{31}P	100.00	1.083×10^4	11.87
^{55}Mn	100.00	6.598×10^3	53.66
^{57}Fe	2.19	8.644×10^2	.08376
^{59}Co	100.00	6.317×10^3	88.80
^{95}Mo	15.72	1.456×10^3	2.756
^{97}Mo	16.53	1.487×10^3	2.872
^{99}Ru	12.72	5.396×10^2	0.1638
^{101}Ru	17.07	1.104×10^3	1.589
^{103}Rh	100.00	8.420×10^2	0.07950
^{183}W	14.40	1.113×10^3	0.1386
^{185}Re	37.50	6.023×10^3	44.98
^{187}Re	62.50	6.085×10^3	45.88
^{187}Os	1.64	6.162×10^2	0.04266
^{189}Os	16.10	2.076×10^3	2.385
^{191}Ir	37.40	4.598×10^2	0.1190
^{193}Ir	62.60	5.007×10^2	0.1410
^{195}Pt	33.80	5.572×10^2	3.525

Table II. Observed Relaxation Rates (R_{obs}) for $[OsH_4(PTol_3)_3]$ in CD_2Cl_2 at Different Fields

nucleus	freq, MHz	B_0, T	T_1(min), ms	R_{obs}, s^{-1}	temp, °C	$10^{10}\tau_c$, s
^1H	500	11.75	221	4.52	−0.7	1.96
^1H	500	11.75	213	4.69	+4.2	1.96
^1H	300	7.05	131	7.63	−22.0	3.26
^1H	300	7.05	127	7.87	−18.6	3.26
^1H	200	4.70	85	11.8	−43	4.90
^{31}P	202	11.75	506	1.98	−50.2	5.66
^{31}P	202	11.75	505	1.98	−49.4	5.66
^2H	61	9.40	11[a]	91	−82.0	15.96

[a] Measured for the deuteride resonance in $[OsD_4\{P(Tol\text{-}o\text{-}d_2)_3\}_3]$.

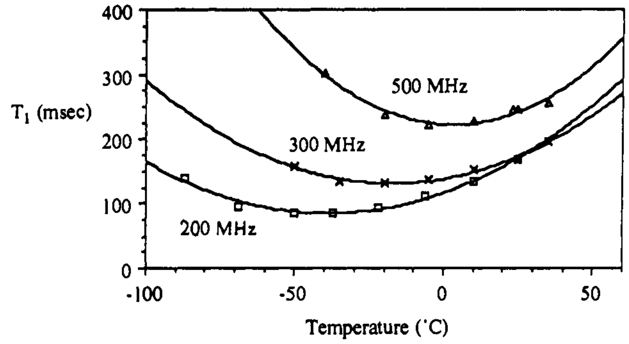

Figure 1. Temperature dependence of T_1 for $[OsH_4(PTol_3)_3]$ in CD_2Cl_2 at different magnetic fields.

---

[10] Abragam, A. *The Principles of Nuclear Magnetism*; Oxford University: New York, 1971; Chapter 8.

[11] Values of γ_X were taken from *CRC Handbook of Chemistry and Physics*.

[12] This assumes that the major contributors to relaxation at the minimum value of T_1 are still ^1H–^1H dipole–dipole interactions since τ_c(min) is not the value of τ_c which makes R_{HX} a minimum. When heteroatom dipole–dipole interactions are the sole contributors to relaxation, the appropriate value of τ_c(min) must be obtained by differentiation of eq 5 with respect to τ_c. Fortunately the difference between the values of K_X, given in Table I, and those evaluated by using values of τ_c(min) derived from differentiation of eq 5 differ by less than 12% for all of the nuclei used in this study.

$$R_{HX} = \frac{2\gamma_H^2\gamma_X^2\hbar^2}{15r^6}S(S+1) \times \left\{\frac{\tau_c}{1+\tau_c^2\omega_-^2} + \frac{3\tau_c}{1+\tau_c^2\omega_H^2} + \frac{6\tau_c}{1+\tau_c^2\omega_+^2}\right\} \quad (5)$$

$$R_{HX} = K_X/r^6 \quad (6)$$

T_1 Measurements on $[OsH_4L_3]$ (L = $PTol_3$, $P(p\text{-}CF_3C_6H_4)_3$, PPh_3, and PMe_2Ph)

The hydride region of the ^1H NMR spectrum of $[OsH_4(PTol_3)_3]$, **1**, consists of a single resonance (δ −7.76, q, J_{HP} = 9 Hz) which at room temperature is a binomial quartet. Plots of T_1 versus temperature for this resonance determined on 200-, 300-, and 500-MHz spectrometers are shown in Figure 1. The values of T_1(min) and R are listed in Table II. Consistent with dipole–dipole relaxation, T_1(min) is proportional to the magnetic field strength (Figure 2). Since relaxation by chemical shift anisotropy increases as the square of the field strength[13] and relaxation by spin rotation is independent of field strength,[14] substantial contributions from either of these mechanisms are precluded.

Measurements of T_1(min) at different magnetic field strengths yielded values of τ_c(min) at three different temperatures. Since τ_c is a molecular property, the values of τ_c(min) at two additional temperatures could be obtained by measurement of T_1(min) of the ^{31}P resonance of $[OsH_4(PTol_3)_3]$, **1** (T_1(min) = 506 ms at 224 K in a field of 11.75 T), and the ^2H resonance of the deuterated analogue $[OsD_4\{P(Tol\text{-}o\text{-}d_2)_3\}_3]$, **1e**. Assuming that the relaxation mechanism is ^1H–^{31}P dipole–dipole interaction, the phosphorus relaxation rate is given by eq 5, where ω_P replaces ω_H in the denominator of the second term. By differentiating with respect to τ_c and setting $\partial R/\partial\tau_c$ equal to zero, the value of τ_c(min) is found to be 5.66×10^{-10} s. For ^2H where the mechanism of relaxation is quadrupole interaction, the value of τ_c(min) can be obtained by replacing ω_H with ω_D in the expression $\omega\tau_c = 0.6158$ (τ_c(min) = 1.596×10^{-9} s when T_1 is a minimum) since the temperature-dependent part of the expression for quadrupole relaxation is the same as that for homonuclear dipole–dipole relaxation. The results of T_1(min) measurements are summarized in Table II.

In accord with the Arrhenius equation, $\tau_c^{-1} = Ae^{-E_a/RT}$, that has been used to describe the temperature dependence of τ_c,[15] the linear plot of $-\ln \tau_c$ vs T^{-1} (Figure 3) yields the activation parameters $A = 5.1 \times 10^{11}$ s and E_a = 2.53 kcal/mol. This is evidence that $[OsH_4(PTol_3)_3]$ behaves isotropically and hence that the relaxation rates can be described by eqs 1 and 5 (more complicated expressions are required to describe the relaxation in unsymmetrical molecules where the three moments of inertia are unequal leading to anisotropic tumbling). Plots of T_1 vs temperature for $[OsH_4(PTol_3)_3]$ in toluene-d_8 and THF-d_8, as well as plots of T_1 vs temperature for $[OsH_5(PTol_3)_3][BF_4]$ and $[K][OsH_3(PTol_3)_3]$ (a static facial octahedron on the basis of the ^1H NMR spectrum which matches those of $[OsH_3(PMe_2Ph)_3^-][K^+]$[16] and $[RuH_3(PPh_3)_3^-][K^+]$[17]), all show similar shapes (Figure 4). This suggests that the rotational correlation time follows Arrhenius-type behavior in these cases as well. In this connection it is worth noting that even when τ_c does exhibit Arrhenius-type behavior, T_1(min) is not the point of intersection of the two lines corresponding to the plots of ln T_1 vs T^{-1}. Near the minimum, the relaxation rate is not a linear function of either τ_c or τ_c^{-1} since the conditions $\omega^2\tau_c^2 \gg 1$ or $\omega^2\tau_c^2 \ll 1$ are no longer satisfied.

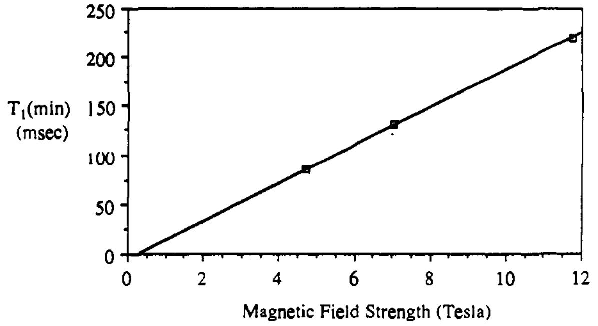

Figure 2. Field dependence of T_1(min) for $[OsH_4(PTol_3)_3]$ in CD_2Cl_2.

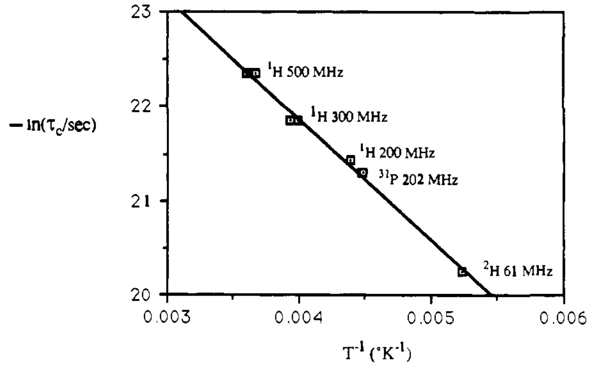

Figure 3. Temperature dependence of τ_c(min) for $[OsH_4(PTol_3)_3]$ in CD_2Cl_2.

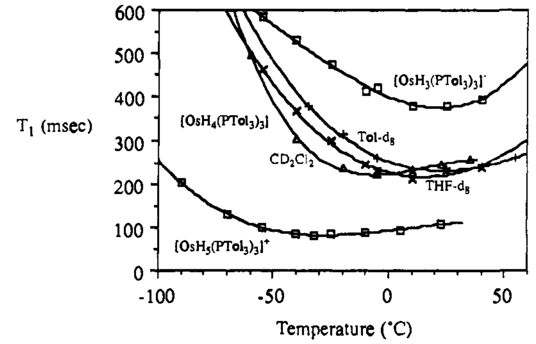

Figure 4. Temperature dependence of T_1 for $[OsH_3(PTol_3)_3]^-$(THF-d_8), $[OsH_4(PTol_3)_3]$(various solvents), and $[OsH_5(PTol_3)_3]^+(CD_2Cl_2)$.

Table III. Observed Relaxation Rates (R_{obs}) for Tris(phosphine)osmium Polyhydrides (at 500 MHz)

compd	solvent	temp, °C	T_1(min), ms	R_{obs}, s^{-1}
$[OsH_4(PTol_3)_3]$	CD_2Cl_2	2[a]	217[a]	4.61[a]
$[OsH_4(PTol_3)_3]$	THF-d_8	10	210	4.76
$[OsH_4(PTol_3)_3]$	$C_6D_5CD_3$	17	232	4.31
$[OsH_4\{P(p\text{-}CF_3C_6H_4)_3\}_3]$	$C_6D_5CD_3$	25	222	4.50
$[OsH_4(PPh_3)_3]$	$C_6D_5CD_3$	2	213	4.69
$[OsH_4(PMe_2Ph)_3]$	$C_6D_5CD_3$	−45	302	3.31
$[OsH_3(PTol_3)_3]^-$	THF-d_8	10	377	2.65
$[OsH_5(PTol_3)_3]^+BF_4^-$	CD_2Cl_2	−32	82	12.2

[a] The average of two independent measurements, T_1(min) = 213 at 4.2 °C and T_1(min) = 221 at −0.7 °C.

The effect of changing the phosphine ligand is shown by the plots of T_1 vs temperature for the series of tetrahydrides $[OsH_4L_3]$ where L = $PTol_3$, $P(p\text{-}CF_3C_6H_4)_3$, PPh_3, and PMe_2Ph (Figure 4). The values of T_1(min) for the triarylphosphine complexes are similar (232, 222, and 213 ms for L = $PTol_3$, $P(p\text{-}CF_3C_6H_4)_3$, and PPh_3, respectively), i.e., some 24–30% lower than T_1(min) for $[OsH_4(PMe_2Ph)_3]$ (302 ms). An increase in relaxation rate with increasing number of phenyl groups also has been observed for other polyhydrides, including $[ReH_5L_3]$, $[ReH_7L_2]$, and $[Re_2H_8L_4]$ (Table VII). As shown subsequently, this can be

---

[13] For relaxation by chemical shift anisotropy, $R_{CSA} = (2/15)\gamma^2B_0^2\Delta\sigma^2\tau_c$.

[14] For relaxation by spin rotation, $R_{SR} = (2\pi IkT/3h)C^2\tau_c$.

[15] For the temperature dependence of τ_c of $[Mn(CO)_5H]$, see: Farrar, T. C.; Quinting, G. R. *J. Phys. Chem.* **1986**, *90*, 2834–2836.

[16] Huffman, J. C.; Green, M. A.; Kaiser, S. L.; Caulton, K. G. *J. Am. Chem. Soc.* **1985**, *107*, 5111–5115.

[17] Chan, A. S. C.; Shieh, H. S. *J. Chem. Soc., Chem. Commun.* **1985**, 1379–1380.

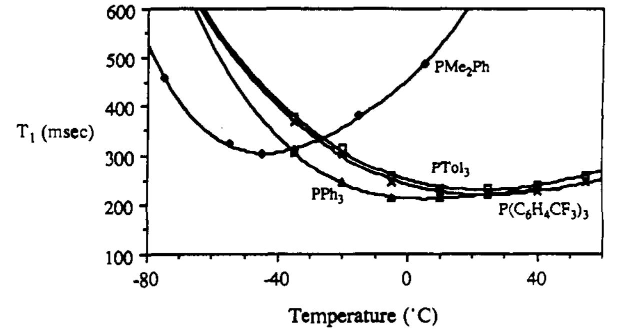

Figure 5. Temperature dependence of T_1 for $[OsH_4(phosphine)_3]$ in toluene-d_8 (effect of changing phosphine).

Table IV. Relaxation Rates for $[OsH_nD_{4-n}\{P(Tol\text{-}d_2)_3\}_3]$, n = 1–4, and $[OsH_4(PTol_3)_3]$ in Toluene-d_8 at 500 MHz and 25 °C

compd	T_1, ms	R_{obs}, s^{-1}
$[OsHD_3\{P(Tol\text{-}o\text{-}d_2)_3\}_3]$ (**1a**)	2090	0.478
$[OsH_2D_2\{P(Tol\text{-}o\text{-}d_2)_3\}_3]$ (**1b**)	749	1.33
$[OsH_3D\{P(Tol\text{-}o\text{-}d_2)_3\}_3]$ (**1c**)	536	1.87
$[OsH_4\{P(Tol\text{-}o\text{-}d_2)_3\}_3]$ (**1d**)	337	2.97
$[OsH_4(PTol_3)_3]$ (**1**)	233	4.29

Scheme I

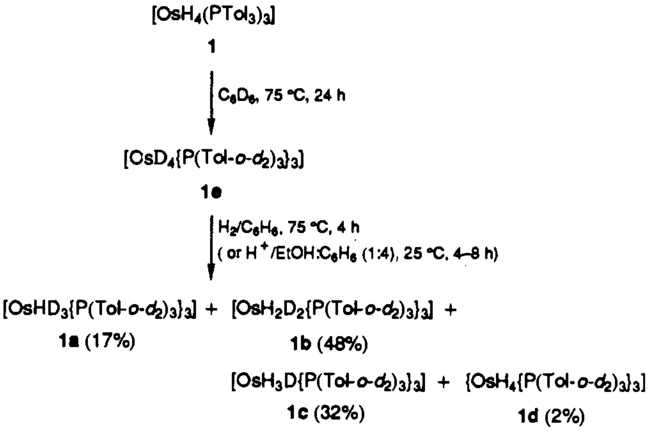

attributed to dipole–dipole interactions between the metal hydrides and o-H atoms of the phosphine ligands. Values of T_1(min) and R_{obs}, measured at 500 MHz for the osmium polyhydrides, are summarized in Table III.

Effect of Deuteration

By extending the approach originally applied by Morris[4b] in a study of $[Fe(\eta^2\text{-}H_2)(H)(dppe)_2]^+$, direct evidence for relaxation by dipole–dipole interactions between ortho protons and metal hydrides was obtained from T_1 measurements on the ortho-deuterated derivatives **1a**–**d**. Each of the four isotopomers, prepared by the exchange reactions shown in Scheme I, gives rise to a distinct resonance in the $^1H\{^{31}P\}$ NMR spectrum (Figure 6). The isotopic perturbation of the chemical shift, +0.013 ppm per D, is similar in magnitude but opposite in sign to that observed in organic molecules[18] and is large enough to allow the T_1 of each isotopomer to be measured independently. Plots of T_1 vs temperature for each of the four isotopomers are shown in Figure 7. Values of T_1 at 298 K are listed in Table IV. The relaxation rate of the monohydride $[OsHD_3[P(Tol\text{-}o\text{-}d_2)_3]_3]$ (**1a**), 0.478 s^{-1}, is almost an order of magnitude smaller than that for the unlabeled compound $[OsH_4(PTol_3)_3]$ (**1**), 4.29 s^{-1}.

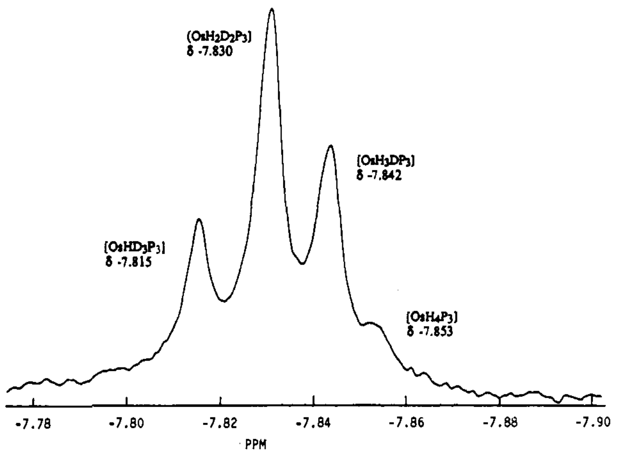

Figure 6. $^1H\{^{31}P\}$ spectrum of the "hydride" region of a C_6D_6 solution of partially deuterated isotopomers of $[OsH_xD_{4-x}\{P(Tol\text{-}d_2)_3\}_3]$.

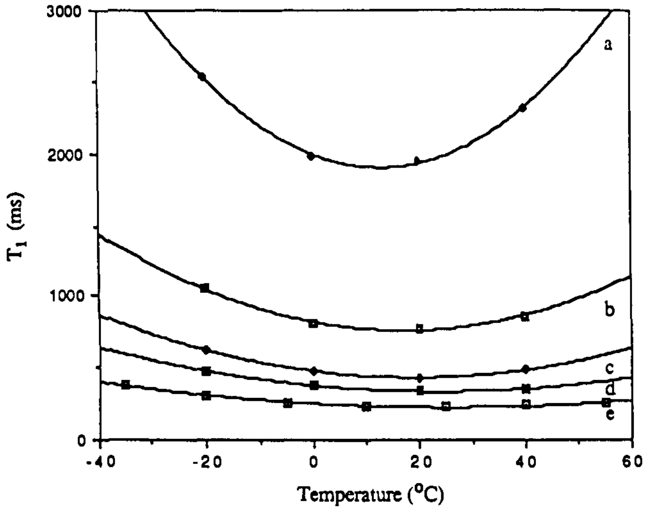

Figure 7. Temperature dependence of T_1 for the isotopomers of $[OsH_xD_{4-x}\{P(Tol_3)_3]$ and $[OsH_4(PTol_3)_3]$: (a) $[OsHD_3\{P(Tol\text{-}d_2)_3\}_3]$ (97% o-D); (b) $[OsH_2D_2\{P(Tol\text{-}d_2)_3\}_3]$ (97% o-D); (c) $[OsH_3D\{P(Tol\text{-}d_2)_3\}_3]$ (99% o-D); (d) $[OsH_4\{P(Tol\text{-}d_2)_3\}_3]$ (99% o-D); (e) $[OsH_4(PTol_3)_3]$.

The observed relaxation rate for the hydrides in $[OsH_4(PTol_3)_3]$, $R_{obs}(\mathbf{1})$, can be expressed as the sum of three contributions: that due to metal hydride–metal hydride dipole–dipole interactions, $R_{H(m)H}$; that due to dipole–dipole interactions with the phosphine ligand ortho protons, $R_{H(l)H}$; and that from all other sources, R_{other} (eq 7). A similar expression can be written for $R_{obs}(\mathbf{1a})$ replacing

$$R_{obs}(\mathbf{1}) = R_{H(m)H} + R_{H(l)H} + R_{other} \qquad (7)$$

the appropriate terms for ^1H–^1H relaxation with corresponding terms for the relaxation due to ^1H–^2H dipole–dipole interactions, $R_{H(m)D}$ and $R_{H(l)D}$ (eq 8). Assuming that the internuclear dis-

$$R_{obs}(\mathbf{1a}) = R_{H(m)D} + R_{H(l)D} + R_{other} \qquad (8)$$

tances determining $R_{H(m)D}$ and $R_{H(m)H}$ are unaffected by isotopic substitution, the ratio of these terms is a constant which can be calculated from eqs 1 and 5. This relation is general and, for measurements made at constant field and temperature, relaxation due to ^1H–^1H dipole–dipole interactions is 15.89 times more rapid than relaxation due to ^2H–^1H dipole–dipole interactions, i.e. $R_{HD} = 0.06293R_{HH}$. Substituting into eq 8 yields eq 9. Assuming

$$R_{obs}(\mathbf{1a}) = 0.06293\{R_{H(m)H} + R_{H(l)H}\} + R_{other} \qquad (9)$$

that R_{other} is the same for all of the isotopmers, subtraction of eq 9 from eq 7, followed by rearrangement, yields eq 10, where the

$$R_{H(m)H} + R_{H(l)H} = 1.067\{R_{obs}(\mathbf{1}) - R_{obs}(\mathbf{1a})\} \qquad (10)$$

left-hand side is the sum of the relaxation rates due to hydride–hydride and hydride–o-H dipole–dipole interactions. With use of the values of R_{obs} from Table IV, the relaxation rate due to

---

[18] Isotopic substitution of hydrogen by deuterium in a methyl group typically results in change in chemical shift of ca. −0.01 ppm per deuterium (Hanson, P. E. *Annu. Rep. NMR Spectrosc.* **1983**, *15*, 105–225).

these interactions is 4.07 s^{-1} which accounts for 95% of the hydride relaxation rate in $[OsH_4(PTol_3)_3]$ (4.29 s^{-1}). Because $[OsHD_3\{P(Tol\text{-}o\text{-}d_2)_3\}_3]$ contains ~0.5% residual protons in the ortho positions,[19] the value of $R_{obs}(\mathbf{1a})$ reported in Table IV is greater than it would be for completely deuterated material. Thus, 4.07 s^{-1} is the minimum contribution to hydride relaxation from ^1H–^1H dipole–dipole interactions in $[OsH_4(PTol_3)_3]$, with all other relaxation mechanisms contributing less than 5%.

The expression for the observed relaxation rate of $[OsH_4\{P(Tol\text{-}o\text{-}d_2)_3\}_3]$ (**1d**) is given by eq 11. Subtraction of eq 11 from eq 7, followed by substitution of $0.06293R_{H(l)H}$ for $R_{H(l)D}$, yields eq 12, where the left-hand side is the relaxation rate due to

$$R_{obs}(\mathbf{1d}) = R_{H(m)H} + R_{H(l)D} + R_{other} \qquad (11)$$

$$R_{H(l)H} = 1.067\{R_{obs}(\mathbf{1}) - R_{obs}(\mathbf{1d})\} \qquad (12)$$

dipole–dipole interactions between the metal hydrides and ortho protons. With use of the values of R_{obs} reported in Table IV, $R_{H(l)H} = 1.41$ s^{-1}, accounting for almost a third of the observed relaxation in $[OsH_4(PTol_3)_3]$. Since $[OsH_4\{P(Tol\text{-}o\text{-}d_2)_3\}_3]$ cannot be prepared without some incorporation of protons into the ortho positions,[20] this value of $R_{H(l)H}$ represents a minimum and the actual contribution to hydride relaxation in $[OsH_4(PTol_3)_3]$ from hydride–o-H dipole–dipole interactions may be greater. However, it is interesting to note that this value is close to the relaxation rate of 1.68 s^{-1} observed for $[OsH(CO)\{P(C_6H_3CH_3)(Tol)_2\}(PTol_3)_2]$ (**2**), a tris(triarylphosphine) *monohydride* complex in which dipole–dipole interactions with the phosphine ligand protons are expected to be the major contributors to hydride relaxation.[21]

Subtracting the contribution from hydride–o-H interactions ($R_{H(l)H} = 1.41$ s^{-1}) from the combined relaxation rate ($R_{H(m)H} + R_{H(l)H} = 4.07$ s^{-1}) yields the relaxation rate due to hydride–hydride dipole–dipole interactions in $[OsH_4(PTol_3)_3]$ ($R_{H(m)H} = 2.66$ s^{-1}). This is within 5% of the relaxation rate calculated by using the hydride–hydride internuclear distances derived from neutron diffraction data on the related complex $[OsH_4(PMe_2Ph)_3]$[23] ($R_{cal} = 2.79$ s^{-1}), consistent with the structures being very similar. By adding the contributions due to hydride–^{31}P (R_{HP}) and hydride–^{189}Os (R_{HM}) dipole–dipole interactions[22] to the contributions due to hydride–hydride ($R_{H(m)H}$) and hydride–o-H interactions ($R_{H(l)H}$), the calculated relaxation rate for $[OsH_4(PTol_3)_3]$ is 4.17 s^{-1} (eq 13) which is within 3% of the experimental

$$\begin{aligned} R_{calc} &= R_{H(l)H} + R_{H(m)H} + R_{PH} + R_{MH} \\ &= 1.41\ s^{-1} + 2.66\ s^{-1} + 0.08\ s^{-1} + 0.02\ s^{-1} = 4.17 s^{-1} \end{aligned} \qquad (13)$$

value. The magnitude of the ligand contribution, $R_{H(l)H}$, reflects short internuclear distances between ortho protons and metal hydrides, also revealed by neutron diffraction studies and consistent with the widespread propensity of triarylphosphine complexes to undergo ortho metalation.[24]

Calculation of Relaxation Rates

The excellent agreement between calculated and observed relaxation rates for $[OsH_4(PTol_3)_3]$ ($R_{obs}/R_{calc} = 1.03$), obtained by including, in addition to the contributions from dipole–dipole interactions from the metal hydrides themselves, interactions with other dipolar nuclei, encouraged us to calculate the relaxation rates for other transition-metal polyhydrides. Since relaxation rates are additive, the total relaxation rate of a given hydride nucleus[8] may be obtained by summing the contributions from the separate dipole–dipole interactions of this nucleus with all other nuclei (eq 14). For fluxional polyhydrides where inequivalent

$$R_{TOT} = \sum_i R_{H(m)H_i} + \sum_i R_{H(l)H_i} + \sum_i R_{HM_i} + \sum_i R_{HP_i} \qquad (14)$$

hydrides are rapidly exchanging, the relaxation rate is the weighted average of the relaxation rate for each type of hydride. For polyhydrides structurally characterized by neutron diffraction, the individual ^1H-X contributions were calculated by means of eqs 4 and 6, using internuclear distances derived from the fractional atomic coordinates. For metals with more than one isotope, the contribution to the relaxation rate due to hydride–metal dipole–dipole interactions, R_{HM}, was assumed to be the weighted sum of the contributions to the relaxation rate calculated for the different metal isotopes. A typical calculation, for $[ReH_5(PMePh_2)_3]$, is described in detail in the Appendix.

For polyhydrides characterized by X-ray crystallography, the hydride–hydride and hydride–metal dipole–dipole contributions to the relaxation rate, $R_{H(m)H}$ and R_{HM}, respectively, were calculated by using the experimental HMH bond angles *and the H–M distances determined from neutron structures on related complexes* (Table VI). The use of H–M distances from neutron diffraction studies on related molecules instead of the fractional atomic coordinates determined by X-ray diffraction is appropriate because of the known tendency of X-ray diffraction data to underestimate H-X distances, leading to artificially high relaxation rates.[6d] The hydride-phosphorus relaxation rate, R_{HP}, was estimated to be 0.027 s^{-1} per phosphorus atom, which is the mean contribution per phosphorus calculated for six different polyhydrides with use of neutron diffraction data (Table V).[25] Where data were available, the phosphine ligand proton contribution to relaxation, $R_{H(l)H}$, was calculated with use of fractional atomic coordinates; in other cases they were estimated by using the approximations described below.

For compounds for which no structural data were available, the relevant hydride–hydride internuclear distances used to calculate $R_{H(m)H}$ were estimated with use of the HMH angles of closely related molecules

Table V. Calculated Contributions to Hydride Relaxation from Phosphine Ligand Atoms

	contribution to hydride relaxation rates, s^{-1}			
compd	$^1H_{ortbo}$	$^1H_\alpha$	$^1H_\beta$	^{31}P
$[WH_6(PPhPr^i_2)_3]$	0.102	0.064	0.052	0.033
$[OsH_4(PMe_2Ph)_3]$	0.076	0.025		0.025
$[ReH_5(PMePh_2)_3]$	0.093	0.048		0.030
$[OsH_6(PPhPr^i_2)_2]$	0.105	0.044	0.051	0.029
$[IrH_5(PPr^i_3)_2]$		0.047	0.060	0.024
$[ReH_7(dppe)]$	0.082	0.019		0.021
mean values	0.092	0.041	0.054	0.027

Table VI. Observed and Estimated Metal Hydride Bond Lengths Used To Calculate Relaxation Rates (Values in Parentheses Are Estimated As Described in the Text)

metal	M–H distance, Å	metal	M–H distance, Å	metal	M–H distance, Å
Ta(V)[37]	1.774	Nb(V)[37]	1.689		
W(IV)	(1.742)	Mo(IV)[39]	1.685		
W(VI)[38]	1.732	Mo(VI)	(1.675)		
				Mn(I)[30]	1.601
Re(III)	(1.697)				
Re(V)[9a]	1.687				
Re(VII)[9b]	1.675				
Os(II)	(1.669)	Ru(II)	(1.593)	Fe(II)[41]	1.529
Os(IV)[23]	1.659	Ru(IV)	(1.583)	Fe(IV)	(1.519)
Os(VI)[40]	1.649	Ru(VI)	(1.573)		
Ir(III)	(1.613)	Rh(III)	(1.532)		
Ir(V)[42]	1.603	Rh(V)	(1.522)		

---

(19) Determined by integration of the resonance due to residual hydrogens in the hydride position relative to the methyl resonance at δ 2.06 ppm.

(20) Although we can measure the amount of ^1H in the ortho positions of the mixture of **1a–1d** (3%) we cannot determine the percent ^1H in the ortho positions of $[OsH_4\{P(Tol\text{-}d_2)_3\}_3]$ alone.

(21) Isolated by column chromatography from the reaction of $[OsH_4(PTol_3)_3]$ with primary or secondary alcohols at 150 °C and characterized by ^1H and $^{31}P\{^1H\}$ NMR spectroscopy. The identity of **2** was confirmed by its reaction with H_2 to give the dihydride $[OsH_2(CO)(PTol_3)_3]$ whose ^1H and $^{31}P\{^1H\}$ NMR spectra are almost identical with that of the known triphenylphosphine analogues.

(22) Calculated with eq 5 and the internuclear distances from the neutron diffraction study of $[OsH_4(PMe_2Ph)_3]$.

(23) Hart, D. W.; Bau, R.; Koetzle, T. F. *J. Am. Chem. Soc.* **1977**, *99*, 7557–7563.

(24) For example, in $[OsH_4(PMe_2Ph)_3]$ two nonbonding interactions between hydrides and ortho protons are reported (H(1)–H(141) = 2.098 Å and H(1)–H(281) = 2.267 Å).[23]

(25) Values range from 0.021 s^{-1} for $[ReH_7(dppe)]$ to 0.033 s^{-1} for $[WH_6(PPhPr^i_2)_3]$.

Table VII. Calculated and Observed Relaxation Rates for Transition-Metal Hydrides for Which Classical Structures Are Assumed (All Values Adjusted to 500 MHz)

		calculated					observed		R_{obs}/R_{calc}	
compd	structural data[a]	$R_{H(m)H}$, s^{-1}	$R_{H(l)H}$,[b] s^{-1}	R_{HM},[c] s^{-1}	R_{HP},[d] s^{-1}	R_{calc}, s^{-1}	R_{obs}, s^{-1}	T_1(min), ms	all contributions	$R_{H(m)H}$ only
$[RuHCp(PPh_3)_2]$		0.00	1.58[e]	0.02	0.05	1.65	1.67[f]	599	1.01	
$[IrH_5(PPr^i_3)_2]$	N	3.70[g]	2.46[g]	0.00[g]	0.05[g]	6.21	1.67[h]	599	0.27	0.45
$[\overline{OsH\{PTol_2(p\text{-}CH_3C_6H_3})\}(CO)(PTol_3)_2]$		0.00	1.56	0.02	0.08	1.66	1.68[h]	595	1.01	
$[OsHCp(PTol_3)_2]$		0.00	1.58	0.02	0.05	1.65	1.78[h]	562	1.08	
$[IrH_2(PPh_3)_2(CO)_2]^+$		0.55	1.10	0.00	0.05	1.70	2.04[k]	490	1.20	3.71
$[ReH_8(PPh_3)]^-$		5.52[l]	0.65	2.07	0.03	8.27	2.04[m]	490	0.25	0.37
$[OsH_3(PTol_3)_3]^-$		0.90	1.66	0.02	0.08	2.66	2.65[h]	377	1.00	2.96
$[OsH_3(PPh_3)_4]^+$	X	0.39[o]	2.21	0.02	0.11	2.73	2.71[p]	369	0.99	6.91
$[WH_6(PMe_2Ph)_3]$		2.92[q]	1.29	0.00	0.08	4.29	2.76[r]	362	0.64	0.94
$[ReHCp_2]$		0.00	0.95[s]	1.91	0.00	2.86	2.86[t]	350	1.00	
$[OsH_3(PTol_3)_4]^+$		0.39[o]	2.21	0.02	0.11	2.73	2.86[h]	350	1.05	7.30
$[MoH_4(PMePh_2)_4]$	X	3.45[u]	1.96	0.04	0.11	5.56	3.03[v]	330	0.54	0.88
$[RuH_3(PPh_3)_3]^-$		1.19[n]	1.66	0.02	0.08	2.95	3.30[h]	303	1.12	2.78
$[OsH_4(PMe_2Ph)_3]$	N	2.79[w]	0.91[w]	0.02[w]	0.08[w]	3.80	3.31[h]	302	0.87	1.19
$[WH_4(dtpe)_2]$		2.73[u]	1.80	0.00	0.11	4.64	3.33[i]	300	0.72	1.22
$[MoH_4(dtpe)_2]$		3.45[u]	1.80	0.04	0.11	5.40	3.49[i]	287	0.65	1.01
$[OsH_4\{P(p\text{-}C_6H_4CF_3)_3\}_3]$		2.79[w]	1.66	0.02	0.08	4.55	4.50[h]	222	0.99	1.61
$[OsH_4(PTol_3)_3]$		2.79[w]	1.66	0.02	0.08	4.55	4.55[h]	220	1.00	1.63
$[OsH_4(PPh_3)_3]$		2.79[w]	1.66	0.02	0.08	4.55	4.69[h]	213	1.03	1.73
$[Re_2H_8(PMe_3)_4]$		2.72[x]	0.74	2.09	0.05	5.60	4.91[y]	204	0.88	1.81
$[Re_2H_8(PMe_2Ph)_4]$		2.72[x]	0.86	2.09	0.05	5.72	5.10[z]	196	0.89	1.88
$[OsH_6(PPhPr^i_2)_2]$	N	4.57[gg]	1.81[gg]	0.02[gg]	0.06[gg]	6.46	5.18[h]	194	0.80	1.13
$[ReH_5(PMe_2Ph)_3]$		3.13[aa]	1.29	1.97	0.08	6.47	5.50[bb]	182	0.85	1.76
$[ReH_3(PMePh_2)_4]$	X	1.12[cc]	2.54[cc]	1.91	0.11	5.68	5.63[dd]	178	0.99	5.05
$[Re_2H_8(PEt_2Ph)_4]$	N	2.72[x]	0.86[x]	2.10[x]	0.07[x]	5.75	5.71[ee]	175	0.99	2.10
$[Re_2H_8(PPh_3)_4]$		2.72[x]	1.10	2.09	0.05	5.96	5.84[ff]	171	0.98	2.15
$[OsH_6(PCy_3)_2]$		4.57[gg]	1.54	0.02	0.05	6.18	6.25[h]	160	1.01	1.37
$[ReH_4(CO)(PMe_2Ph)_3]^+$		3.32[hh]	1.29	1.97	0.08	6.66	6.25[ii]	160	0.94	1.89
$[ReH_5(PMePh_2)_3]$	N	3.13[aa]	1.55[aa]	1.97[aa]	0.09[aa]	6.74	6.65[jj]	150	0.99	2.12
$[ReH_5(PPh_3)_3]$	X	3.02[ll]	1.27[ll]	1.97	0.08	6.34	5.80–8.70[kk]	114–172	0.91–1.37	1.92–2.88
$[ReH_7(dppe)]$	N	6.44[mm]	0.74[mm]	2.07[mm]	0.04[mm]	9.29	7.46[nn]	134	0.80	1.16
$[ReH_7(PPh_3)_2]$		6.44[mm]	1.10	2.07	0.05	9.66	9.09[oo]	110	0.94	1.41
$[ReH_7\{P(C_6H_4F)_3\}_2]$		6.44[mm]	1.10	2.07	0.05	9.66	9.09[pp]	110	0.94	1.41

[a] Structural characterization: N = neutron diffraction; X = X-ray diffraction. [b] Calculated with eq 15. [c] Calculated with the equation, $R_{HM} = \sum a_i K_{Mi}(r_{HM})^{-6}$, where a_i is the natural abundance of isotope M_i, K_{Mi} has the value given in Table I, and r_{HM} is the HM internuclear distance (Table VI). [d] Calculated with the equation $R_{HP} = n0.027\ s^{-1}$, where n is the number of phosphorus atoms. [e] The sum of the contributions from twelve ortho hydrogens and one cyclopentadiene ($R_{H(l)H} = 12 \times 0.092\ s^{-1} + 0.474\ s^{-1}$). [f] At 250 MHz, T_1(min) = 300 ms.[3a] [g] Calculated with internuclear distances from the neutron diffraction study of $[IrH_5(PPr^i_3)_3]$.[42] [h] This work. [i] Reference 44. [j] Calculated assuming cis hydrides ($\phi_{HMH} = 90°$). [k] At 250 MHz, T_1(min) = 245 ms.[3a] [l] Calculated with the hydride–hydride internuclear distances reported in the neutron diffraction study of $[ReH_9]^{-}$[43] and replacing one of the capping hydrogens by phosphorus. [m] At 250 MHz, T_1(min) = 245 ms.[3a] [n] Calculated assuming an idealized octahedral structure of facial hydrides ($\phi_{HMH} = 90°$). [o] Calculated assuming that the hydrides cap three faces of the tetrahedron formed by the four phosphines. For the X-ray structure of $[OsH_3(PPh_3)_4]^+$ see ref 36. [p] At 400 MHz, T_1(min) = 245 ms.[48] [q] Calculated with the internuclear distances from the neutron diffraction structure of $[WH_6P(PhPr^i_2)_3]$.[38] [r] At 250 MHz, T_1(min) = 181 ms.[3a] [s] Estimated as described in ref 27. [t] At 400 MHz, T_1(min) = 280 ms.[6d] [u] Calculated with the HMH angles in $[MoH_4(PMePh_2)_4]$ as determined by X-ray crystallography.[45] [v] At 250 MHz, T_1(min) = 165 ms.[3a] [w] Calculated with the internuclear distances reported in the neutron diffraction study of $[OsH_4(PMe_2Ph)_3]$.[23] [x] Calculated with the internuclear distances reported in the neutron diffraction study of $[Re_2H_8(PEt_2Ph)_4]$.[46] [y] At 400 MHz, T_1(min) = 163 ms.[6d] [z] At 400 MHz, T_1(min) = 157 ms.[6d] [aa] Calculated with the internuclear distances reported in the neutron diffraction study of $[ReH_5(PMePh_2)_3]$.[9a] [bb] At 400 MHz and −80 °C, two resonances are observed, δ −6.3 (2 H, T_1(min) = 151 ms) and δ −7.2 (3 H, T_1(min) = 140 ms).[6a] The value reported is the weighted average corrected to 500 MHz. [cc] Calculated with internuclear distances in $[ReH_3(PMePh_2)_4]$ as determined by X-ray crystallography.[6b] Hydride–hydride distances were calculated with the experimental bond angles and the bond length reported in Table VI. [dd] At 400 MHz, T_1(min) = 142 ms.[6b] [ee] At 400 MHz, T_1(min) = 140 ms.[6d] [ff] At 400 MHz T_1(min) = 137 ms.[6d] [gg] Calculated with the internuclear distances reported in the neutron diffraction study of $[OsH_6(PPr^i_2Ph)_2]$.[40] [hh] Calculated assuming a distorted tetrahedral geometry. The smallest HMH angle was taken to be 69°, the angle reported for the adjacent hydrides in $[ReH_3(PMePh_2)_4]$.[6b] [ii] At 250 MHz, T_1(min) = 80 ms.[47] [jj] Below −20 °C two resonances are observed, δ −5.8 (2 H, T_1(min) = 96 ms, 400 MHz and −40 °C) and δ −6.6 (3 H, T_1(min) = 140 ms, 400 MHz and −60 °C).[6a] The value reported is the weighted average corrected to 500 MHz. [kk] T_1(min) = 138 ms at 400 MHz in toluene-d_8, 117 ms at 400 MHz in CD_2Cl_2, and 46 ms at 200 MHz in acetone-d_6.[6a] [ll] Calculated with the internuclear distances from the X-ray structure of $[ReH_5(PPh_3)_3]$.[6a] Hydride–hydride distances were calculated with the experimental bond angles and the bond length reported in Table VI. [mm] Calculated with the internuclear distances reported in the neutron diffraction study of $[ReH_7(dppe)]$.[9b] [nn] At 250 MHz, T_1(min) = 67 ms.[3a] [oo] At 500 MHz, T_1(min) = 110 ms.[3a] [pp] At 250 MHz, T_1(min) = 55 ms.[3a]

as determined by neutron or X-ray crystallography and the M–H bond distances listed in Table VI.[26] R_{HM} and R_{HP} were calculated as described above for compounds characterized by X-ray crystallography. The contributions for each of the different types of hydride–ligand proton interactions were estimated with eq 15, where the constants 0.092 s^{-1} per

$$R_{H(l)H} = 0.092n_{ortho} + 0.041n_\alpha + 0.054n_\beta \qquad (15)$$

o-H, 0.041 s^{-1} per α-H, and 0.054 s^{-1} per β-H are the mean values calculated from neutron diffraction data on six transition-metal polyhydrides (Table V) and n_{ortho}, n_α, and n_β are the number of ortho, α, and β protons, respectively. The contribution from the protons attached to a cyclopentadienyl ligand was estimated to be 0.474 s^{-1} per cyclopentadienyl.[27] The procedures followed in each case are detailed in the footnotes to Tables VII–IX.

---

(26) Determined by neutron diffraction studies on other transition-metal hydrides of the same metal or estimated by extrapolation. For third-row transition-metal hydrides the M–H internuclear distance decreases on going left to right across the periodic table (Δr = −0.051 ± 0.016 Å per unit increase in nuclear charge at constant number of electrons) and with increasing oxidation state (Δr = −0.005 ± 0.001 Å per unit increase in atomic charge at constant nuclear charge). X-ray data on first- and second-row transition-metal hydrides exhibit a similar decrease in metal–hydride bond length going left to right across the periodic table (Δr = −0.046 Å per unit increase in nuclear charge). Teller, R. G.; Bau, R. *Struct. Bonding* **1981**, *44*, 1–82.

Table VIII. Internuclear Distances Calculated from the Observed Relaxation Rates for Nonclassical Transition-Metal Polyhydrides (Values in Parentheses Calculated Assuming Rapid Rotation of the η^2-H_2 Ligand)

compd	type of H	R_{obs}, s^{-1}	R_{cal}, s^{-1}	r_{HH}, Å fast rotation	r_{HH}, Å slow rotation
$Os(H_2)(OEP)$	η^2-H_2	6.96^a		1.19	1.49
$[Os(H_2)H(depe)_2]^+$	η^2-H_2	9.9^b		1.17	1.48
	H	2.17^c	2.49^p		
$[OsH_2(PPh_3)_3(\eta^2$-$OAc)]^+$	η^2-H_2	20^o		1.01	1.27
$[Re(H_2)H_4(Cyttp)]^+$		19^d	25^e (14)	0.91	1.14
$[Ru(H_2)H(dppe)_2]^+$	η^2-H_2	40^f		0.89	1.13
	H	2.75^g	2.08^p		
$[Fe(H_2)H(dppe)_2]^+$	η^2-H_2	47^h	267^i (68)	0.87	1.09
	H	3.48^j	3.38^i		
$[Ir(H_2)H(bq)(PCy_3)_2]^+$	η^2-H_2	60^k		0.83	1.05
$[Re(H_2)H_2(CO)$-$(PMe_2Ph)_3]^+$	η^2-H_2	60^l		0.84	1.05
	H	5.4^m	4.95^q		
$[RuCp(H_2)(CO)$-$(PCy_3)]^+$	η^2-H_2	120^n		0.74	0.93

[a] At 400 MHz, $T_1(\min)$ = 115 ms.[7c] [b] At 400 MHz, $T_1(\min)$ = 81 ms.[4b] [c] At 400 MHz, $T_1(\min)$ = 369 ms.[4b] [d] At 250 MHz, $T_1(\min)$ = 27 ms.[7b] [e] Calculated with the internuclear distances determined by X-ray diffraction.[7b] [f] At 400 MHz, $T_1(\min)$ = 20 ms.[4b] [g] At 400 MHz, $T_1(\min)$ = 291 ms.[4b] [h] At 400 MHz, $T_1(\min)$ = 17 ms.[4b] [i] Calculated with the internuclear distances determined by neutron diffraction.[2d] [j] At 400 MHz, $T_1(\min)$ = 230 ms.[4b] [k] At 250 MHz, $T_1(\min)$ = 8 ms.[52] [l] At 250 MHz, $T_1(\min)$ = 8 ms.[47] [m] At 250 MHz, $T_1(\min)$ = 90 ms.[48] [n] At 250 MHz, $T_1(\min)$ = 4 ms.[52] [o] At 400 MHz, $T_1(\min)$ = 41 ms.[48] [p] Calculated with the HMH angles from the neutron diffraction study of $[Fe(\eta^2\text{-}H_2)(H)(dppe)_2][BPh_4]$.[2c] [q] The HMH angle between terminal hydrides was assumed to be the same as that reported for $[ReH_3(PMePh_2)_4]$.[6b]

"Classical" Hydrides

Table VII lists the calculated and observed relaxation rates (R_{calc} and R_{obs}, respectively) for complexes inferred to have classical structures on the basis of diffraction studies of the same or closely related molecules or from ^1H NMR spectra (for example, both $[RuH_3(PPh_3)_3]^-$ and $[OsH_3(PPh_3)_3]^-$ exhibit AA′A″XX′X″ resonances in the hydride region characteristic of octahedral configurations with a facial arrangement of hydrides).[28] Also listed are the ratios of relaxation rates (R_{obs}/R_{cal}) as well as the corresponding ratios obtained assuming, as has commonly been done prior to this, that hydride–hydride interactions are the only contributors to relaxation (i.e., $R_{cal} = R_{H(m)H}$). For most of the polyhydrides examined, the calculated and observed relaxation rates agree to within 10%, suggesting that the time-averaged solution structures closely resemble the solid-state structures and that dipole–dipole interactions are the main contributors to hydride relaxation. The polyhydrides for which the difference between calculated and observed exceeds 20% fall into two classes, (1) polyhydrides which depart substantially from spherical symmetry and consequently are expected to exhibit significantly anisotropic behavior in solution ($[IrH_5(PPr^i_3)_2]$, $[ReH_8(PPh_3)]^-$, $[WH_6(PMe_2Ph)_3]$, and $[ReH_7(dppe)]$), and (2) the eight-coordinate tetrahydrides $[MoH_4(PMePh_2)_4]$, $[MoH_4(dppe)_2]$, and $[WH_4(dppe)_2]$.

For the former group, the discrepancies cannot be due wholly to differences between the solution and solid-state geometries since for $[IrH_5(PPr^i_3)_2]$ and $[ReH_7(dppe)]$ all possible arrangements of the hydride ligands yield calculated relaxation rates that are substantially greater than the observed ones. Nor can it be due to overestimation of non-hydride dipole–dipole contributions, since for $[IrH_5(PPr^i_3)_2]$, even when such contributions are neglected, the calculated relaxation rate still is larger than the observed one, 1.67 s^{-1} (unless the two phosphines are assumed to be sterically inactive so that the hydrides form a trigonal bipyramid; for this geometry $R_{H(m)H}$ is 1.66 s^{-1}). The most probable explanation for the discrepancies between calculated and observed relaxation rates for these polyhydrides is that they exhibit anisotropic behavior in solution. The equations used to calculate the relaxation rates reported in Table VII (eq 1 and 5) are applicable only to molecules tumbling isotropically in solution. When the three moments of inertia are unequal, the relaxation rate cannot be calculated with a single rotational correlation time as required by eqs 1 and 5. For a symmetric top such as $[IrH_5(PPr^i_3)_2]$ where $I_z < I_x = I_y$ (a crude calculation of moments of inertia ignoring the contributions from hydrogen atoms yields $I_z/I_x = 0.41$), the observed relaxation rate is predicted to be less than the value calculated assuming isotropic tumbling.[29] The same arguments can be applied to $[ReH_8(PPh_3)]^-$, $[WH_6(PMe_2Ph)_3]$, and $[ReH_7(dppe)]$.

The discrepancies between observed and calculated relaxation rates for the eight-coordinate tetrahydrides, $[MoH_4(PMePh_2)_4]$, $[MoH_4(dppe)_2]$, and $[WH_4(dppe)_2]$, are more difficult to rationalize. They are unlikely to be due to anisotropic tumbling since the X-ray structure reported for $[MoH_4(PMePh_2)_4]$[45] reveals a pseudo tetrahedral arrangement of both phosphines and hydrides that make it unlikely that the three moments of inertia are significantly different. Since the phosphorus and metal contributions to relaxation (R_{HP} and R_{HM}) are small, and the approximations used to calculate the ligand contributions ($R_{H(l)H}$) work well for other complexes, the most probable source of error is the hydride–hydride contribution, $R_{H(m)H}$. The average HMH angle between adjacent hydrides in $[MoH_4(PMePh_2)_4]$ as determined by X-ray crystallography is 60.7°. Agreement between calculated and observed relaxation rates for $[WH_4(dppe)_2]$, $[MoH_4(dppe)_2]$, and $[MoH_4(PMePh_2)_4]$ may be obtained by using angles of 69°, 72°, and 81°, respectively.

Omitting these two classes of molecules, the average value of R_{obs}/R_{cal} for 26 hydrides is 0.98 ± 0.08. *This increases to 2.50 if only hydride–hydride interactions are considered.* Thus, on average, about 60% of the hydride relaxation rate in these polyhydrides arises from contributions other than hydride–hydride dipole–dipole interactions. Although R_{HP} is small in all cases, $R_{H(l)H}$ and R_{HM} can be substantial contributors to hydride relaxation. This was noted earlier by Cotton et al., who estimated the rhenium dipole contribution to hydride relaxation by measuring the relaxation rate of $[Cp_2ReH]$ ($T_1(\min)$ = 280 ms at 400 MHz).[6d] A recent paper which considers only hydride–hydride interactions when calculating $T_1(\min)$ notes that the difference between calculated and observed values is exceptionally large for the dimeric polyhydride $[Re_2H_8(PEt_2Ph)_4]$ (302 ms calculated vs 140 ms observed at 400 MHz).[3d] This discrepancy disappears (R_{obs}/R_{cal} = 0.99) when other contributions are considered, the largest of which is the contribution due to hydride–rhenium dipole–dipole interactions (R_{HRe} = 2.10 s^{-1}). Since four of the hydrides in this molecule are bridging and accordingly interact with two rhenium nuclei, the hydride–rhenium interactions account for 37% of the total relaxation rate. Even for the mononuclear complexes $[ReH_5(PMePh_2)]$ and $[ReH_7(dppe)]$, the rhenium contributions to hydride relaxation are substantial, 30% and 28%, respectively. Large hydride–metal dipole–dipole contributions to relaxation also can be expected for hydrides bound to cobalt

---

(27) Estimated by assuming that the difference between R_{obs} and R_{ReH} for $ReCp_2H$[6d] is equal to $R_{H(l)H}$ (2.859 s^{-1} − 1.911 s^{-1} = 0.948 s^{-1}). This lies between the value of 1.468 s^{-1} calculated with the ligand proton-hydride internuclear distances found in $Cp(C_2H_5Cp)ReH$ after the hydride position is adjusted to bisect the dihedral angle (ϕ = 161.6°) formed by the planes of the two cyclopentadienyl rings (Paciello, R. A.; Kiprof, P.; Herdtweck, E.; Herrmann, W. A. *Inorg. Chem.* **1989**, *28*, 2890–2893) and the value of 0.668 s^{-1} calculated assuming the dihedral angle between cyclopentadienyl ligands is 135°, the value predicted for $ReCp_2H$ in a theoretical study of bis(cyclopentadienyl) compounds (Lauher, J. W.; Hoffmann, R. *J. Am. Chem. Soc.* **1976**, *98*, 1729–1735).

(28) Only the compounds $[ReH_8(PPh_3)]^-$, $[IrH_2(CO)_2(PPh_3)_2]^+$, and $[ReH_4(CO)(PMePh_2)_3]^+$ cannot be identified as classical by these criteria. For the first two compounds the relaxation rates are so low that there is little doubt about their assignment as classical structures ($T_1(\min)$ = 490 ms). In the last case the classical structure is supported by the identification of a nonclassical isomer (Table VIII).

(29) For a more detailed explanation see: Woessner, D. E. *J. Chem. Phys.* **1962**, *37*, 647–654.

Table IX. Range of the Shortest Hydride–Hydride Internuclear Distance Consistent with the Observed Relaxation Rates in Various Geometries (Values in Parentheses Are Calculated Neglecting Contributions to Hydride Relaxation from Nuclei Other Than Hydrides)

compd	R_{obs}, s^{-1}	structure[a]	r_{HH}, Å	
			fast rotation	slow rotation
$[RhH_2\{P(CH_2CH_2PPh_2)_3\}]^+$	0.94[b]		(1.66)	(2.09)
[*rac*-$Os(H_2)H$(tetraphos)]$^+$	5.0[c]	*fac*-MH_3		1.90 (1.77)
		trans-$M(\eta^2\text{-}H_2)H$ (E)	1.26 (1.17)	1.59 (1.48)
$[RuH_4(PCy_3)_3]$	11[d]	MH_4 (B)		1.56 (1.49)
		$M(\eta^2\text{-}H_2)H_2$ (F)	1.04 (0.99)	1.32 (1.26)
$[OsH_5(PTol_3)_3]^+$	12[e]	MH_5 (C)		1.58 (1.54)
		$M(\eta^2\text{-}H_2)H_3$ (G)	0.99 (0.96)	1.26 (1.22)
$[RuH_6(PCy_3)_2]$	14[f]	MH_6 (D)		1.57 (1.54)
		$M(\eta^2\text{-}H_2)H_4$ (H)	0.97 (0.94)	1.22 (1.18)
		$M(\eta^2\text{-}H_2)_2H_2$ (I)	1.04 (1.01)	1.31 (1.28)
$[OsH_5(PPh_3)_3]^+$	14[g]	MH_5 (C)		1.53 (1.50)
		$M(\eta^2\text{-}H_2)H_3$ (G)	0.95 (0.93)	1.21 (1.18)
$[ReH_2(PMePh_2)_4Cl]$	16[h]		1.08 (1.03)	1.37 (1.30)
$[IrH_6(PCy_3)_2]^+$	18[i]	MH_6 (D)		1.50 (1.47)
		$M(\eta^2\text{-}H_2)H_4$ (H)	0.89 (0.87)	1.21 (1.17)
		$M(\eta^2\text{-}H_2)_2H_2$ (I)	0.98 (0.96)	1.23 (1.21)
$[RuH_4(PPh_3)_3]$	26[e]	MH_4 (B)		1.30 (1.29)
		$M(\eta^2\text{-}H_2)H_2$ (F)	0.86 (0.85)	1.09 (1.08)
$[RuH_5(PPh_3)_3]^+$	56[e]	MH_5 (C)		1.20 (1.19)
		$M(\eta^2\text{-}H_2)H_3$ (G)	0.73 (0.73)	0.91 (0.91)

[a] Letters in parentheses refer to the structures in Figures 8 and 9. [b] At 80 MHz, T_1 = 170 ms.[49] [c] At 400 MHz, T_1 = 160 ms.[50]. [d] At 200 MHz, T_1 = 36 ms.[4a] [e] This work. [f] At 200 MHz, T_1 = 28 ms.[4a] [g] At 250 MHz, T_1 = 35 ms.[3a] [h] At 200 MHz, T_1 = 25 ms.[2e] [i] The weighted average of the relaxation rates of the signals observed at −80 °C. At 500 MHz, T_1 = 48 (4 H) and 73 ms (2 H), respectively.[51]

and manganese. Indeed the ^{55}Mn dipole contribution to hydride relaxation in $[MnH(CO)_5]$ (R_{HMn} = 2.941 s^{-1} at 500 MHz) has been used to calculate the Mn–H bond length.[15] The internuclear distance calculated from T_1(min), 1.65 ± 0.05 Å, agrees well with the bond length determined by neutron diffraction, 1.60 Å.[30]

The contribution to R_{calc} from phosphine protons also can be quite large as demonstrated by our deuterium substitution experiments. Further evidence for this is provided by the short hydride–*o*-H distances revealed by neutron diffraction. As expected the relative importance of these contributions is greatest for the mono-, di-, and trihydrides (in $[OsH_3(PTol_3)_4]^+$, hydride interactions with phosphine ligand protons account for 79% of the observed relaxation rate), but even for the hexahydride $[OsH_6(PCy_3)_2]$, where the hydride–hydride contributions may be expected to dominate, more than 25% of the observed relaxation rate can be accounted for by dipole–dipole interactions between the hydrides and phosphine ligand protons.

"Nonclassical" Polyhydrides

The hydrides treated in this section have been demonstrated to have "nonclassical" structures (i.e. to contain η^2-H_2 ligands) by one or more of the following: (a) neutron or X-ray diffraction, (b) "static" NMR spectra, (c) H–D coupling constants, or (d) infrared spectroscopy (measurement of ν_{HH}). The comparison of calculated and observed relaxation rates for such hydrides is complicated by (1) the sensitivity of the relaxation rate to η^2-H_2 internuclear distance, (2) rotation of the η^2-H_2 ligand which can increase the observed relaxation time by a factor of 4 in the limit of fast rotation,[4a,31] and (3) the limited number of structurally characterized η^2-H_2 complexes for which T_1(min) has been measured. Because of the r^{-6} dependence, the relaxation rate is extremely sensitive to small changes in *r*. Thus, increasing r_{HH} from 0.82 to 0.89 Å, the range of H–H distances determined by neutron diffraction, decreases R_{HH} from 255 to 156 s^{-1}. For nonclassical polyhydrides of unknown structure, the relaxation rates of the η^2-H_2 ligands may be used to calculate the η^2-H_2 H–H separations with use of eq 16 in which $R(H_N\text{–}H_N)$ is the relaxation

$$R(H_N\text{–}H_N) = \alpha\,\{R_{obs}(H_N) - R(H_N\text{–}H_C) - R(H_N\text{–}H_L) - R(H_N\text{–}P) - R(H_N\text{–}M)\} \quad (16)$$

rate *due only to the dipole–dipole interaction between the two protons of the η^2-H_2 ligand*. This is obtained by subtracting from the relaxation rate of the η^2-H_2 protons ($R_{obs}(H_N)$) the contributions due to interactions of the η^2-H_2 protons with phosphine ligand protons ($R(H_N\text{–}H_L)$), with phosphorus atoms ($R(H_N\text{–}P)$), with metal atoms ($R(H_N\text{–}M)$, and with any terminal hydrides ($R(H_N\text{–}H_C)$). These terms were calculated as described for classical polyhydrides. For fluxional molecules where exchange between classical and nonclassical sites averages the relaxation rates and prevents a direct measurement of $R_{obs}(H_N)$, the latter is obtained by using eq 17 where $R(H_C)$ is the average relaxation

$$mR(H_N) = \{(m + n)R_{obs} - nR(H_C)\} \quad (17)$$

rate of the terminal hydrides calculated as before, *n* is the number of terminal hydrides, and *m* is the number of nonclassical hydrides. Since relaxation rates can be affected by rotation of the η^2-H_2 ligand, the observed relaxation rate is consistent with a range of internuclear distances. Table VIII lists the ranges of η^2-H_2 internuclear distances consistent with the observed relaxation rates in the limit of both fast (α = 4) and slow (α = 1) rotation of the η^2-H_2 ligand compared with rotation of the molecule (eq 16).

While the observed relaxation rate for $[ReH_6(Cyttp)]^+$[8b] (R_{obs} = 19 s^{-1}) lies within the range of relaxation rates calculated with use of internuclear distances determined by crystallography (R_{calc} = 14–25 s^{-1}), this is not the case for $[Fe(H_2)H(dppe)_2]^+$ where the observed relaxation rate (R_{obs} = 47 s^{-1}) is more than 35% smaller than the relaxation rate calculated in the limit of fast rotation. Thus, the time averaged η^2-H_2 internuclear distance in solution must be at least 0.05 Å longer than that in the solid at 20 K. Except for $[Ru(H_2)H(dppe)_2]^+$, there is generally good agreement (R_{obs}/R_{calc} = 1.0 ± 0.13) between the calculated and observed relaxation rates of the terminal hydrides suggesting that the relaxation processes in nonclassical polyhydride complexes are similar to those in classical ones and that exchange between classical and nonclassical sites is slow compared with relaxation.

The observed relaxation rates for the nonclassical polyhydride complexes are of interest for several reasons. First, they demonstrate that there is considerable overlap between the values of T_1(min) for classical and nonclassical hydrides. For $[Os(\eta^2\text{-}H_2)OEP]$[8b] the relaxation rate of the η^2-H_2 ligand (6.96 s^{-1}) is well within the range found for classical hydrides (Table VIII). Second, they show that the range of internuclear distances in η^2-H_2 ligands, consistent with the observed values of T_1(min), is quite large (from 0.74 Å in $[RuCp(\eta^2\text{-}H_2)(CO)(PCy_3)^+]$ to 1.49 Å in $[Os(\eta^2\text{-}H_2)OEP]$). Third, they show that even for the hydrogen nuclei in η^2-H_2 ligands, contributions to relaxation from dipole–

---

(30) La Placa, S. J.; Hamilton, W. C.; Ibers, J. A.; Davison, A. *Inorg. Chem.* **1969**, *8*, 1928–1933.

(31) Eckert, J.; Kubas, G. J.; Dianoux, A. J. *J. Chem. Phys.* **1988**, *88*, 466–474.

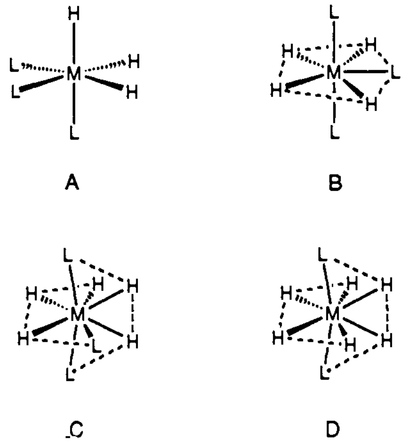

Figure 8. Idealized geometries for classical polyhydrides: (A) octahedron, (B) pentagonal bipyramid, (C) dodecahedron (cf. $[ReH_5(PMePh_2)_3]$ structure), and (D) dodecahedron (cf. $[OsH_6(PPr^i_3)_2]$ structure).

dipole interactions other than hydride–hydride interactions may be significant. Thus 25% of the observed relaxation rate of the η^2-H_2 ligand in $[Os(\eta^2\text{-}H_2)H(depe)_2]^{+}$ [8b] is due to interactions with phosphine ligand protons. The previously reported range of internuclear distances (1.12 ± 0.03 to 1.40 ± 0.03 Å), calculated assuming (a) that the dipole–dipole interaction between nuclei in the η^2-H_2 ligand is the only contributor to relaxation and (b) a relaxation rate of 2.5 s^{-1} for the terminal hydride, is significantly smaller than the range reported here (1.17–1.48 Å).

Polyhydrides of Unknown Structure

For compounds of unknown structure, the internuclear distances consistent the observed relaxation times were calculated for both classical and nonclassical configurations. For the former case, the calculations assume the geometries of closely related polyhydrides deduced from X-ray or neutron diffraction studies (Figure 8). The internuclear distances between all adjacent hydrides were defined by a single average angle between adjacent hydrides, α, and $R_{H(m)H}$ was calculated as a function of that angle. The internuclear distances reported in Table IX are those that satisfy eq 18. The values in parentheses are those calculated assuming

$$R_{H(m)H} = R_{obs} - R_{H(l)H} - R_{HP} - R_{HM} \qquad (18)$$

$R_{H(m)H} = R_{obs}$ (i.e., neglecting contributions to hydride relaxation other than hyride–hydride dipole–dipole interactions).

The geometries used to calculate internuclear distances for nonclassical structures are depicted in Figure 9. The geometries corresponding to the shortest η^2-H_2 internuclear distance are those that minimize the interactions with the terminal hydrides. Taking account of rotation of the η^2-H_2 ligand leads to a range of η^2-H_2 internuclear distances. These were calculated by means of eq 16, using the values $R(H_N–H_N)$ deduced as described in the preceding section, and are reported in Table IX.

For many of the compounds in Table IX, including some (e.g., $[RuH_4(PCy_3)_3]$ and $[rac\text{-}Os(H_2)H(tetraphos)^+]$[8b]) that have previously been characterized as η^2-H_2 complexes on the basis of the "T_1 criterion", the values of T_1 are, in fact, compatible with structures in which hydride–hydride internuclear distances exceed 1.50 Å, i.e., *with classical structures*. Thus, for $[OsH_5(PTol_3)_3^+]$, the observed relaxation rate is consistent with structures in which the shortest H–H separation is as long as 1.58 Å (classical) or as short as 0.99 Å (nonclassical). Similar results are obtained for $[RuH_4(PCy_3)_3]$, $[RuH_6(PCy_3)_2]$, and $[IrH_6(PCy_3)_2^+]$. This illustrates a major limitation of "T_1 criterion", namely, that while structure uniquely defines T_1(min), T_1(min) does not uniquely define structure. A given value of T_1(min) is consistent with an infinite array of geometries, and if these include both classical and nonclassical structures, T_1(min) cannot be used to distinguish between them. For example, although T_1(min) for $[ReH_7(PPh_3)_2]$ (110 ms at 500 MHz) is within 6% of the value calculated assuming the classical structure found by neutron diffraction for the dppe analogue, this agreement cannot be used to rule out alternative structures, including nonclassical ones. Thus, the shortest hydride–hydride internuclear distance would have to be decreased from 1.77 to 1.20 Å before R_{cal} and R_{obs} would differ by 20%. (**Added in Proof**: A recent neutron diffraction structure determination of $[RuH_7(PTol_3)_2]$ reveals a "short" H···H contact of 1.357 Å, consistent with the above. On the basis of this structure, $T_1(\text{min})_{calc}$ = 93 ms in the limit of slow rotation or 124 ms in the limit of fast rotation, compared with $T_1(\text{min})_{obs}$ = 110 ms for $[ReH_7(PPh_3)_2]$ and $[ReH_7(P\{C_6H_4F\}_3)_2]$ (Brammer, L.; Howard, J. A. K.; Johnson, O.; Koetzle, T. F.; Spencer, J. L.; Stringer, A. M. *J. Chem. Soc., Chem. Commun.* **1991**, 241–243).

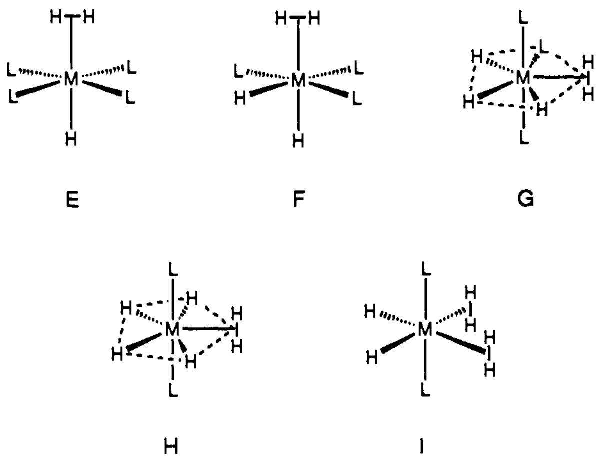

Figure 9. Idealized geometries for nonclassical polyhydrides: (E, F, I) octahedra, (G, H) pentagonal bipyramid.

Conclusions

The following features of this study are noteworthy. (1) Evidence is provided that dipole–dipole interactions are the main contributors to hydride relaxation for a large number of polyhydrides, even those for which there are no short ^1H–^1H internuclear distances characteristic of η^2-H_2 ligands. (2) It is shown that for many polyhydrides, T_1(min) can be calculated to within a few percent by using internuclear distances obtained from neutron or X-ray diffraction studies *provided that dipole–dipole interactions with ligand and metal nuclei are included*. In many cases such interactions are the major contributors to hydride relaxation. (3) It is shown that for some polyhydrides, the observed values of T_1(min) are consistent with both classical and nonclassical structures. Many earlier attempts to apply the "T_1 criterion" to distinguish between classical and nonclassical polyhydride structures suffer from two severe shortcomings, namely (a) failure to take account of interactions of the hydride ligands with other nuclei and (b) assigning nonclassical structures without ruling out classical ones that may also be consistent with observed T_1 values. Despite this, as the results of this study bear out, where carefully applied and correctly interpreted, T_1 measurements can provide valid and useful structural information about transition-metal polyhydrides.

Experimental Section

All manipulations were performed under an inert atmosphere of nitrogen or argon with standard air-sensitive techniques. THF, hexane, pentane, ether, and benzene were freshly distilled from sodium benzophenone under nitrogen. Dichloromethane was dried over calcium hydride and distilled from P_2O_5. Ethanol was dried by distillation from calcium oxide. Deuterated solvents were dried by stirring over calcium hydride under nitrogen for at least 24 h, degassed by 3 freeze–pump–thaw cycles, and distilled under vacuum. PMe_2Ph, $PTol_3$, and $P(p\text{-}CF_3C_6H_4)_3$ were obtained from Strem Chemical Co. and used without further purification. $[OsO_4]$ was obtained from Johnson Matthey Co. $[OsCl_6^{2-}][NH_4^+]_2$,[32] $[OsH_4(PPh_3)_3]$,[33] $[K][OsH_3(PPh_3)_3]$,[34] and

---

[32] Dwyer, F. P.; Hogarth, J. W. *Inorg. Synth.* **1957**, *5*, 206–207.

[33] Ahmad, N.; Levison, J. J.; Robinson, S. D.; Uttley, M. F. *Inorg. Synth.* **1974**, *15*, 56–57.

$[OsH_4(PMe_2Ph)_3]$[35] were prepared according to literature procedures. NMR samples were prepared with standard air-sensitive techniques and sealed under vacuum or dihydrogen. NMR measurements were made on GE Omega 500, GE Omega 300, and Varian 200 spectrometers. The standard inversion recovery sequence 180–τ–90 was used to determine T_1. Values of T_1 were obtained from the slopes of linear plots of ln ($I_\infty - I_\tau$) vs τ where I_∞ is the peak intensity at $\tau = \infty$. Independent measurements on identical samples gave values of T_1 reproducible to within 2%. Values of T_1(min) and the temperature at which it occurs are accurate to ±5% and ±5 °C, respectively.

$[OsH_4(PTol_3)_3]$ (1) was prepared by the same procedure as the triphenylphosphine analogue,[33] using tri-*p*-tolylphosphine in place of triphenylphosphine, and purified by column chromatography on silica gel. Eluting with 95/5 hexanes/ether gave two fractions, the first containing free tri-*p*-tolylphosphine and the second pure **1**. Removal of the solvent under reduced pressure yielded analytically pure compound as a white solid in 76% yield. ^1H NMR (C_6D_6): ∂ 7.58 (m, 18 H, ortho), 6.77 (d, J_{HH} = 8 Hz, 18 H, meta), 2.06 (s, 27 H, methyl), −7.76 (quartet, J_{PH} = 9 Hz, 4 H, hydride). $^{31}P\{^1H\}$ NMR (C_6D_6): ∂ 20.8 (s). Anal. Calcd: C, 68.33; H, 6.10. Found: C, 69.08; H, 6.66.

$[OsH_4\{P(C_6H_4CF_3)_3\}_3]$ was prepared as above, using tris(*p*-(trifluoromethyl)phenyl)phosphine. The crude material, precipitated from the reaction mixture, was washed with water, ethanol, and pentane and dried under vacuum at room temperature to give a 65% yield of the product as a white powder. ^1H NMR (C_6D_6): ∂ 7.16 (m, 18 H, ortho), 7.11 (d, J_{HH} = 8 Hz, 18 H, meta), −8.02 (quartet, J_{PH} = 9 Hz, 4 H, hydride). $^{31}P\{^1H\}$ NMR (C_6D_6): ∂ 18.8 (s). Anal. Calcd: C, 47.50; H, 2.53. Found: C, 44.23; H, 2.28.

$[OsH_5(PTol_3)_3][BF_4]$. A rapidly stirred solution of **1** in dichloromethane (0.10 M) was cooled to −78 °C under an atmosphere of dihydrogen. One equivalent of trifluoromethanesulfonic acid or tetrafluoroboric acid in diethyl ether (0.020 M) was added by syringe. The reaction was immediate and quantitative by $^{31}P\{^1H\}$. Although the product isolated by precipitation with ether or pentane was contaminated by varying amounts of $[OsH_3(PTol_3)_4{}^+][BF_4{}^-]$[36] pure product could be obtained by removal of the solvents at low temperature. Material isolated in this manner showed no evidence of impurities by either ^1H or $^{31}P\{^1H\}$ NMR although rapid decomposition at room temperature in the absence of hydrogen precluded elemental analysis. ^1H NMR (CD_2Cl_2): ∂ 6.85 (m, 36 H, aryl), 2.27 (s, 27 H, methyl), −5.85 (quartet, J_{PH} = 4 Hz). $^{31}P\{^1H\}$ NMR (CD_2Cl_2): ∂ 7.24 (s).

$[OsD_4\{P(Tol\text{-}o\text{-}d_2)_3\}_3]$ (1e). A Schlenk flask containing 100 mg of $[OsH_4(PTol_3)_3]$ and fitted with a high-vacuum stopcock was attached to a high-vacuum line and evacuated. Benzene-d_6 (5 mL) was added by vacuum distillation and the flask was sealed. After being heated to 75 °C for 12 h the solvent was removed under vacuum. Fresh benzene-d_6 (5 mL) was added to the white solid and the solution was heated to 75 °C for an additional 12 h. Removal of the solvent under vacuum yielded a product enriched to 99.5% d-atom in the hydride sites as shown by integration of the residual resonance in the hydride region against the methyl resonance of the phosphine ligands.

$[OsH_4D_{4-n}\{P(Tol\text{-}o\text{-}d_2)_3\}_3]$ Isotopomers (1a–d). A Schlenk flask containing 100 mg of $[OsD_4\{P(Tol\text{-}o\text{-}d_2\}_3]$ and fitted with a high-vacuum stopcock was attached to a high-vacuum line and evacuated. Benzene (5 mL) was added by vacuum distillation and the solution was degassed by 3 freeze–pump–thaw cycles and stirred under 1 atm of hydrogen at room temperature. The flask was sealed and heated to 75 °C for 4 h. Removal of the solvents under vacuum left a white powder which was found to contain a 0.17/0.48/0.32/0.02 mixture of mono- (**1a**), di- (**1b**), tri- (**1c**), and tetrahydride (**1d**) by integration of the hydride resonances in the $^1H\{^{31}P\}$ NMR spectrum (Figure 6). Integration of the meta and ortho resonances showed greater than 92% d-atom in the ortho position.

$[OsH_6(PPr^i{}_2Ph)_2]$.[40] A Schlenk flask containing 0.64 g of $Na_2[OsCl_6]$ and fitted with a high-vacuum stopcock was attached to a high-vacuum line and evacuated. Degassed ethanol (100 mL) and $[PPr^i{}_2Ph]$ (0.70 mL) were added by syringe. The mixture was heated to reflux and a degassed solution of $[NaBH_4]$ (0.74 g) in ethanol (36 mL) was added over a period of about 10 min during which the color changed from dark green to pale yellow. The solution was refluxed for another 5 min, stirred overnight, cooled in a salt–ice bath for 3 h, and filtered under N_2. The solvent was removed by evaporation at room temperature under vacuum. The residue was washed twice with degassed water (40 mL) and extracted with degassed hexane. The extract was dried over Na_2SO_4 and passed through a 12-cm column of neutral Al_2O_3. After eluting with hexane, nitrogen was passed through the hexane solution to reduce the volume to ca. 5 mL and degassed ethanol (5 mL) was added. Cooling to 0 °C resulted in precipitation of the product. $^{31}P\{^1H\}$ NMR (CD_2Cl_2): δ 53.5 (s, 2 P). ^1H NMR (CD_2Cl_2): δ 8.0 (br s, 4 H), 7.4 (m, 6 H), 2.3 (m, 4 H), 1.10 (dd, 12 H, J = 15.5, 6.5 Hz), 0.88 (dd, J = 14.5, 7.5 Hz, 12 H), −9.8 (t, J_{PH} = 9.4 Hz, H).

Table X. Calculated Internuclear Distances in $[ReH_5(PMePh_2)_3]$ (Å)

	Unit Cell Parameters			
a	17.9350 Å		α	91.7200°
b	20.0660 Å		β	100.6400°
c	10.4030 Å		γ	69.4800°

	HT11	HT12	HT13	HT14	HT15
			Hydride–Hydride		
HT11	0.000	1.974	1.847	3.071	3.016
HT12	1.974	0.000	3.156	3.164	3.139
HT13	1.847	3.156	0.000	2.045	2.054
HT14	3.071	3.164	2.045	0.000	1.834
HT15	3.016	3.139	2.054	1.834	0.000
			Hydride–Ortho Hydrogen		
H3	6.332	4.902	6.285	5.158	4.428
H7	5.228	4.737	4.211	2.298	2.990
H9	3.999	2.509	4.876	3.997	4.838
H13	6.613	5.252	6.342	4.434	5.093
H16	3.606	4.647	4.442	5.256	6.176
H20	3.878	5.041	2.606	2.849	4.042
H22	5.160	5.155	5.626	5.173	6.709
H26	2.479	2.053	4.159	4.570	4.922
H29	5.162	4.651	5.916	6.540	5.062
H33	4.710	4.388	4.055	3.775	2.125
H35	3.293	4.535	2.010	3.445	2.393
H39	4.740	5.309	5.203	6.568	5.047
			Hydride–Methyl Hydrogen		
H1A	5.681	3.835	6.191	5.136	4.837
H1B	4.654	3.084	5.216	4.694	3.846
H1C	4.378	2.436	5.329	4.714	4.487
H14A	4.659	4.157	4.494	3.037	4.735
H14B	4.451	4.461	3.669	2.423	4.246
H14C	4.941	5.062	4.716	3.842	5.611
H27A	3.291	2.568	4.672	5.309	4.451
H27B	2.433	2.893	3.933	5.183	4.440
H27C	3.884	3.943	5.002	6.119	4.915
			Hydride–Phosphorus		
P11	3.863	2.436	3.951	2.679	2.740
P12	2.473	2.801	2.707	2.485	3.789
P13	2.496	2.640	2.915	3.777	2.417
			Hydride–Rhenium		
Re1	1.676	1.697	1.679	1.700	1.691

---

(34) Bruno, J. W.; Huffman, J. C.; Green, M. A.; Caulton, K. G. *J. Am. Chem. Soc.* **1984**, *106*, 8310–8312.

(35) (a) Douglas, P. G.; Shaw, B. L. *J. Chem. Soc. A* **1970**, 334–338. (b) Bell, B.; Chatt, J.; Leigh, G. J. *J. Chem. Soc., Dalton Trans.* **1973**, 997–1004.

(36) Sidle, A. R.; Newmark, R. A.; Pignolet, L. H. *Inorg. Chem.* **1986**, *25*, 3412–3418.

(37) Wilson, R. D.; Koetzle, T. F.; Hart, D. W.; Kvick, A.; Tipton, D. L.; Bau, R. *J. Am. Chem. Soc.* **1977**, *99*, 1775–1781.

(38) Gregson, P.; Mason, S. A.; Howard, J. A. K.; Spencer, J. L.; Turner, D. G. *Inorg. Chem.* **1984**, *23*, 4103–4107.

(39) Schultz, A. J.; Stearley, K. L.; William, J. M.; Mink, R.; Stucky, G. D. *Inorg. Chem.* **1977**, *16*, 3303–3307.

(40) Howard, J. A. K.; Johnson, O.; Koetzle, T. F.; Spencer, J. L. *Inorg. Chem.* **1987**, *26*, 2930–2933.

(41) The average of the terminal Fe–H distances reported for $[Fe(H_2)(\eta^2\text{-}H_2)(PEtPh_2)_3]$[2d] and $[Fe(H)(\eta^2\text{-}H_2)(dppe)_2][BPh_4]$.[2b]

(42) Garlaschell, L.; Kahn, S. L.; Bau, R.; Longoni, G.; Koetzle, T. F. *J. Am. Chem. Soc.* **1985**, *107*, 7212–7213.

(43) Abrahams, S. C.; Ginsberg, A. P.; Knox, K. *Inorg. Chem.* **1964**, *3*, 558–567.

(44) Nevitt, I.; Halpern, J. Unpublished results.

(45) Meakin, P.; Guggenberger, L. J.; Peet, W. G.; Muetterties, E. L.; Jesson, J. P. *J. Am. Chem. Soc.* **1973**, *95*, 1467–1474.

(46) Bau, R.; Carroll, W. E.; Teller, R. G.; Koetzle, T. F. *J. Am. Chem. Soc.* **1977**, *99*, 3872.

(47) Luo, X.-L.; Crabtree, R. H. *J. Chem. Soc., Chem. Commun.* **1990**, 189–190.

(48) Siedle, A. R.; Newmark, R. A.; Korba, G. A.; Pignolet, L. H.; Boyle, P. D. *Inorg. Chem.* **1988**, *27*, 1593–1594.

(49) Bianchini, C.; Mealli, C.; Peruzzini, M.; Zanobini, F. *J. Am. Chem. Soc.* **1987**, *109*, 5548–5549.

(50) Bautista, M. T.; Earl, K. A.; Maltby, P. A.; Morris, R. H. *J. Am. Chem. Soc.* **1988**, *110*, 4056–4057.

Table XI. Calculated Contributions to Hydride Relaxation from $^1H-^1H$ Dipole–Dipole Interactions in $[ReH_5(PMePh_2)_3]$

	HT11	HT12	HT13	HT14	HT15	R_{av}
Hydride Contribution						
HT11	0.000	1.310	1.952	0.092	1.103	
HT12	1.310	0.000	0.078	0.077	0.081	
HT13	1.952	0.078	0.000	1.060	1.032	
HT14	0.092	0.077	1.060	0.000	2.037	
HT15	0.103	0.081	1.032	2.037	0.000	
$R_{H(m)H}$	3.457	1.547	4.122	3.266	3.253	3.129
Ortho Contribution						
H3	0.001	0.006	0.001	0.004	0.010	
H7	0.004	0.007	0.014	0.526	0.108	
H9	0.019	0.311	0.006	0.019	0.006	
H13	0.001	0.004	0.001	0.010	0.004	
H16	0.035	0.008	0.010	0.004	0.001	
H20	0.023	0.005	0.247	0.145	0.018	
H22	0.004	0.004	0.002	0.004	0.001	
H26	0.334	1.035	0.015	0.009	0.005	
H29	0.004	0.008	0.002	0.001	0.005	
H33	0.007	0.011	0.017	0.027	0.842	
H35	0.061	0.009	1.175	0.046	0.413	
H39	0.007	0.003	0.004	0.001	0.005	
$R_{H(1)H}$ ortho	0.501	1.410	1.496	0.799	1.419	1.125
Methyl Contribution						
H1A	0.002	0.024	0.001	0.004	0.006	
H1B	0.008	0.090	0.004	0.007	0.024	
H1C	0.011	0.371	0.003	0.007	0.009	
H14A	0.008	0.015	0.009	0.099	0.007	
H14B	0.010	0.008	0.032	0.383	0.013	
H14C	0.005	0.005	0.007	0.024	0.002	
H27A	0.061	0.270	0.007	0.003	0.010	
H27B	0.373	0.132	0.021	0.004	0.010	
H27C	0.023	0.021	0.005	0.001	0.005	
$R_{H(1)H}$ methyl	0.501	0.936	0.090	0.533	0.088	0.430

Table XII. Calculated Contributions to Hydride Relaxation in $[ReH_5(PMePh_2)_3]$ from $^1H-^{31}P$, $^1H-^{185}Re$, and $^1H-^{187}Re$ Dipole–Dipole Interactions

	HT11	HT12	HT13	HT14	HT15	R_{av}
Phosphorus Contribution						
P11	0.004	0.057	0.003	0.032	0.028	
P12	0.052	0.025	0.030	0.050	0.004	
P13	0.049	0.035	0.019	0.004	0.060	
R_{HP}	0.104	0.116	0.053	0.087	0.092	0.090
Rhenium Contribution						
185Re (37.5%)	0.757	0.702	0.749	0.695	0.718	
187Re (62.5%)	1.295	1.200	1.282	1.189	1.228	
R_{HRe}	2.052	1.903	2.031	1.884	1.946	1.968
Total Relaxation						
R_{cal}	6.615	5.911	7.791	6.566	6.797	6.742

where $R_{cal} = R_{H(m)H} + R_{H(1)Hortho} + R_{H(1)Hmethyl} + R_{HP} + R_{HRe}$

$[OsH_6\{PCy_3\}_2]$. $(NH_4)_2[OsCl_6]$ (383.5 mg) and PCy_3 (1.0 g) were placed in a 3-necked flask fitted with a condenser and gas inlet. The flask was evacuated and flushed with N_2 three times. Degassed ethanol (50 mL) was added and the mixture was heated to reflux. A degassed solution of $NaBH_4$ (0.55 g) in ethanol (30 mL) was added and heating was continued for another 10 min. The mixture was stirred overnight and the solvent was removed by evaporation at room temperature under vacuum. The residue was washed with water, cold ethanol, and cold pentane (3 × 10 mL each) and the product was dried under vacuum; yield 200 mg (48%, not optimized). $^{31}P\{^1H\}$ NMR (CD_2Cl_2): δ 41.1 (s). ^1H NMR (CD_2Cl_2): δ 2.0 (d, J = 11.6 Hz, 12 H), 1.81 (br s, 12 H), 1.64 (m, 12 H), 1.38 (quasi, q, J = 11.6 Hz, 12 H), 1.24 (quasi t, J = 5.8 Hz, 18 H). $^{13}C\{^1H\}$ (CD_2Cl_2): δ 40.1 (t, J_{PC} = 14.8 Hz), 30.7 (s), 28.3 (t, J_{PC} = 5.2 Hz), 27.5 (s).

Addendum

Subsequent to the completion of this study and preparation of this manuscript a paper appeared[52] that touches in part on some of the same issues as this one, notably the calculation of T_1(min) for several hydrides of known structure and comparison with experimental values. An independent assessment of the information in ref 52 leads to conclusions that support those of the present paper. Reference 52 compares, for some 13 hydrides, among which both classical and nonclassical structures are represented, experimental values of T_1 with those calculated *assuming only hydride–hydride interactions*, i.e., those corresponding to $[R_{H(m)H}]^{-1}$ of the present paper. Only for two of the five classical hydrides treated in ref 52 ($[ReH_5(PPh_3)_3]$ and $[WH_6(PMePh_2)_3]$) can it be concluded that the agreement between these values is within 10%. For several of the other hydrides the calculations yield a fairly extensive range of values so that the comparisons do not provide a very severe test. Furthermore, for at least three of the cases where good agreement is claimed, namely $[ReH_7(dppe)]$, and $[ReH_5(PMePh_2)_3]$, and $[ReH_5(PPh_3)_3]$, there is reason to believe that this agreement is fortuitous (see below).

The neglect of interactions with other nuclei clearly is not justified in the light of the results of the present paper, even for some of the cases treated in ref 52, for example $[ReH_7(dppe)]$, $[ReH_5(PMePh_2)_3]$, $[Re_2H_8(PEt_2Ph)_4]$, and $[ReH_5(PPh_3)_3]$, where such interactions account for 29%, 55%, 51%, and ca. 50%, respectively, of the total relaxation rate. The discrepancy between the observed and calculated values of T_1(min) for $[ReH_8(PEt_2Ph)_4]$ already has been discussed in the text. Other cases are discussed below.

$[ReH_7(dppe)]$. The apparently good agreement obtained by ignoring the contributions of nuclei other than the metal-coordinated protons is likely due to the fact that anisotropic tumbling in solution decreases the observed relaxation rate by enough to offset the neglect of the rhenium and ligand contributions to relaxation.

$[ReH_5(PMePh_2)_3]$. Although the same theory and equations (notably eq 1 of ref 52 which reduces to $R = 77.6r^{-6}$ at 500 MHz in agreement with eq 4 of this paper) are used in ref 52 and in this paper, the results of the two calculations are, for some cases, most markedly for $[ReH_5(PMePh_2)_3]$, quite disparate. Thus for this case our calculations, reported in Table VII and described in detail in the Appendix, yield a value of $R_{H(m)H} = 3.13\ s^{-1}$ corresponding to T_1(min) of 319 ms at 500 MHz or 255 ms at 400 MHz, in contrast to the "calculated value of 156 ms" cited in ref 52. The value that we calculate is in much poorer agreement with the experimental value of 120 ms at 400 MHz. Only by including interactions with the Re nucleus and with the ligand protons can reasonable agreement between calculated and experimental values of T_1(min) be achieved in this case.

$[ReH_5(PPh_3)_3]$. Cotton et al.[6d] recently have called attention to the disparity between the calculated T_1(min) value (148 ms at 400 MHz)[3d] for $[ReH_5(PPh_3)_3]$ obtained by using H···H distances derived from X-ray crystallographic Re–H distances (1.54 Å) and the T_1(min) value (259 ms at 400 MHz) obtained by using, instead, M–H distances derived from the neutron structure of $[ReH_5(PMe_2Ph)_3]$. The former is in good agreement with the experimental value of 138 ms[6a] whereas the latter is not. The discrepancy is attributed to underestimation of the M–H distance by X-ray crystallography which measures the position of the centroids of electron density rather than that of the proton. Thus, in this case also, it appears that the claimed agreement between the calculated and the observed T_1(min) value is fortuitous, reflecting accidental cancellation of the errors resulting from underestimation of the H···H separation and neglect of the contributions to hydride relaxation from the Re and ligand nuclei. When the latter are included (Table VII) the calculated value of T_1(min) (using neutron M–H distances) becomes 117 ms at 400 MHz (147 msec at 500 MHz) in agreement with the experimental value of 117 ms in acetone-d_6 at 400 MHz.[6c]

Acknowledgment. We are grateful to the National Science Foundation for support of this research, to Prof. Terry Raines and

---

(51) Crabtree, R. H.; Lavin, M. *J. Chem. Soc., Chem. Commun.* **1985**, 1661–1662.

(52) Luo, X.-L.; Crabtree, R. H. *Inorg. Chem.* **1990**, *29*, 2788–2791.

Tom Doman for computational assistance, to Dr. Sergio Deganello and Prof. Robert Bau for assistance with the calculations of internuclear distances, to Giulia Gulia for a sample of $[IrH_5(PPr^i_3)_2]$, and to Johnson Matthey for a generous loan of osmium.

Appendix: Calculation of the Hydride Relaxation Rate in $[ReH_5(PMePh_2)_3]$

Using the unit cell parameters and fractional atomic coordinates determined by neutron diffraction,[9a] the internuclear distances, r_{HX}, between each of the five hydrides and all other dipolar nuclei, including other hydrides, ortho hydrogens, methyl hydrogens, phosphorus, and rhenium nuclei in $[ReH_5(PMePh_2)_3]$ were calculated by means of eq 19, where a, b, c, α, β, and γ are the unit cell parameters and Δx, Δy, and Δz are the differences between the fractional atomic coordinates of the two nuclei (Table X). (Meta and para proton are neglected because their contributions to the hydride relaxation rate are negligible.)

$$r_{\mathrm{HX}} = \{(a\Delta x)^2 + (b\Delta y)^2 + (c\Delta z)^2 + 2ab\Delta x\Delta y \cos\gamma + 2ac\Delta x\Delta z \cos\beta + 2bc\Delta y\Delta z \cos\alpha\}^{0.5} \quad (19)$$

Contributions to the relaxation rates from the individual dipole–dipole interactions were calculated as follows. For proton–proton interactions, the relaxation rate is calculated by using eq 4, where r_{HH} is the internuclear distance between the two protons (Å). The sum of the relaxation rates for interaction of hydride HT11 with each of the four other hydride nuclei yields the contribution to the relaxation of HT11 resulting from dipole–dipole interactions with the other hydrides, $R_{\mathrm{H(m)H}}$. $R_{\mathrm{H(m)H}}$ was calculated for each of the five hydrides and these terms were averaged to yield the average hydride–hydride contribution to the hydride relaxation rate. The contributions to hydride relaxation from hydride–ortho hydrogen, and hydride–methyl hydrogen dipole–dipole interactions were calculated similarly (Table XI).

$$R_{\mathrm{HH}} = \frac{77.51\ \text{Å}^6\ \mathrm{s}^{-1}}{(r_{\mathrm{HH}})^6} \quad (4)$$

Contributions to hydride relaxation due to hydride–phosphorus dipole–dipole interactions were calculated by using eq 20, where r_{HP} is the P–H internuclear distance (Å). Again the interactions of a given hydride with all three phosphorus nuclei were summed to give the total relaxation rate, R_{HP}, for each hydride. These five terms were summed and divided by five to give the average contribution to hydride relaxation due to phosphorus–hydride dipole–dipole interactions (Table XII).

$$R_{\mathrm{HP}} = \frac{11.87\ \text{Å}^6\ \mathrm{s}^{-1}}{(r_{\mathrm{HP}})^6} \quad (20)$$

The contribution to hydride relaxation due to hydride–rhenium dipole–dipole interactions was calculated by using eq 21, where the first term represents the relaxation arising from ^{1}H–^{185}Re interactions (37.5% natural abundance) and the second term represents the relaxation arising from ^{1}H–^{187}Re interactions (62.5% natural abundance). Again the relaxation rates, R_{HRe}, for each hydride were summed and divided by five to obtain the average rhenium–hydride contribution to relaxation (Table XII).

$$R_{\mathrm{HR}}\mathrm{e} = 0.375\left(\frac{44.98\ \text{Å}^6\ \mathrm{s}^{-1}}{(r_{\mathrm{HRe}})^6}\right) + 0.625\left(\frac{45.88\ \text{Å}^6\ \mathrm{s}^{-1}}{(r_{\mathrm{HRe}})^6}\right) \quad (21)$$

The calculated relaxation rate for the hydride ligands in $[ReH_5(PMePh_2)_3]$ is the sum of the contributions from all the nuclei, i.e., other hydrides, ortho hydrogens, methyl hydrogens, phosphorus, and rhenium (eq 22).

$$\begin{aligned} R_{\mathrm{cal}} &= R_{\mathrm{H(m)H}} + R_{\mathrm{H(l)H}}(\mathrm{ortho}) + R_{\mathrm{H(l)H}}(\mathrm{Me}) + R_{\mathrm{HP}} + R_{\mathrm{HR}}\mathrm{e} \\ &= 3.129\ \mathrm{s}^{-1} + 1.125\ \mathrm{s}^{-1} + 0.430\ \mathrm{s}^{-1} + 0.090\ \mathrm{s}^{-1} + 1.968\ \mathrm{s}^{-1} = 6.742\ \mathrm{s}^{-1} \end{aligned} \quad (22)$$

Intrinsic Binding Properties of a Differentiated Iron Subsite in Analogues of Native $[Fe_4S_4]^{2+}$ Clusters

John A. Weigel and R. H. Holm*

Contribution from the Department of Chemistry, Harvard University, Cambridge, Massachusetts 02138-2902.

Received December 24, 1990

Abstract: The cubane-type clusters $[Fe_4S_4(LS_3)L']^{z-}$ (**3**; LS_3 = 1,3,5-tris((4,6-dimethyl-3-mercaptophenyl)thio)-2,4,6-tris(*p*-tolylthio)benzene(3−)) contain $[Fe_4S_4]^{2+}$ core units whose iron subsites are differentiated in the ratio 3:1. In the first extensive study of its kind, the intrinsic binding affinities at the unique subsite toward a large variety of biological and abiological ligands have been examined in Me_2SO solutions. The clusters $[Fe_4S_4(LS_3)Cl]^{2-}$ (**4**) and $[Fe_4S_4(LS_3)(OC_6H_4\text{-}p\text{-}Br)]^{2-}$ (**18**), which have been isolated, undergo subsite-specific, usually stoichiometric, substitution reactions with free ligands and trimethylsilyl reagents, respectively. A set of some 30 clusters of type **3** with four-, five-, and six-coordinate subsites have been generated in situ from **4** and **18**. These reactions can be monitored by ^{1}H NMR owing to the extreme sensitivity of ligand isotropic shifts to the identity of ligand L′ at the unique subsite. The ligands RS^-, RO^-, CN^-, and N_3^- afford four-coordinate subsites, while certain chelating ligands lead to five- and six-coordinate subsites. Among the clusters produced are those that simulate the binding of Tyr·O^-, Ser·O^-, Asp/Glu·CO_2^-, one or two Cys·S^-, and three His·Im protein side chain groups and the solvated and deprotonated (hydroxide) forms of native clusters. Ligand binding reactions are accompanied by changes in $[Fe_4S_4]^{2+/1+}$ redox potentials, which provide another means of detecting product clusters and convey the sign of the intrinsic potential shift upon variation of ligands at the unique subsite. These results are pertinent to the reaction chemistry of native subsite-differentiated clusters such as that in aconitase, which in the resting state exists with H_2O/OH^- at the unique subsite.

Introduction

The function of the all-cysteinate ligated cluster **1** as an electron transfer center in ferredoxin (Fd) proteins and in enzymes is widely recognized. However, it is now evident that electron transfer is not the sole biological function of Fe_4S_4 clusters. Among the most significant recent developments in iron–sulfur biochemistry is the recognition of a class of enzymes that contain Fe–S clusters and no other prosthetic groups and catalyze *nonredox* transformations. Of these, the only one for which interpretation of active site structure and reaction pathway has been reduced to a molecular level is aconitase.[1,2] This enzyme is an isomerase, catalyzing the

---

(1) Beinert, H.; Kennedy, M. C. *Eur. J. Biochem.* **1989**, *186*, 5.

0002-7863/91/1513-4184$02.50/0